Contribution of the Rumen Epithelial Transcriptome and Microbial Community to Variation in Beef Cattle Feed Efficiency

by

Rebecca Kong

A thesis submitted in partial fulfillment of the requirements for the degree of

Master of Science

in

Animal Science

Department of Agricultural, Food and Nutritional Science

University of Alberta

ABSTRACT

Feed efficient cattle consume less feed and produce less environmental waste than inefficient cattle. Many factors are known to contribute to differences in feed efficiency. However, it is unknown how the rumen epithelium and its associated microorganisms influence the feed efficiency of cattle. Our study aimed to understand how host gene expression in the rumen epithelium and the activity of rumen epithelial attached microbes contribute to differences in feed efficiency. Residual feed intake (RFI) of 175 Hereford x Angus steers was measured using a GrowSafe system. The rumen epithelial transcriptome from 9 of the most efficient (low (L-) RFI) and 9 of the most inefficient (high (H-) RFI) steers was obtained using RNA-seq. Differential gene expression analysis was conducted using DESeq2 software and Weighted Gene Co-expression Network Analysis (WGCNA) was performed to identify gene modules that are correlated with RFI. Additionally, we identified and quantified the relative abundance of bacterial and archaeal 16S rRNA transcripts as an indication of their activity. Within the rumen epithelium there were 122 genes that were differentially expressed between L- and H- RFI steers ($p<0.05$). Also, WGCNA identified a significant module of 764 genes that negatively correlated with RFI ($r=-0.5$, $p=0.03$). Functional analysis revealed up-regulation of genes in the L-RFI epithelium involved in modulation of intercellular adhesion, cell migration, cytoskeletal organization, protein and cell turnover, oxidative phosphorylation, and acetylation. Our results suggest the increased tissue morphogenesis in the L-RFI epithelium may increase epithelial paracellular permeability for the absorption of nutrients. Up-regulation of oxidative phosphorylation and acetylation in the L-RFI epithelium indicate potential increased energy production to support the energetic demands of increased tissue morphogenesis in feed efficient animals. There was no significant difference between RFI groups in the activity of archaeal

phylotypes on the epithelium. However, the bacterial families *Campylobacteraceae* and *Neisseriaceae* had significantly greater activity on the L-RFI epithelium ($p<0.05$) and they play a role in oxygen scavenging. Overall, L-RFI (efficient) steers may have increased rumen tissue morphogenesis that possibly increase paracellular permeability for the absorption of nutrients, thereby providing a greater substrate supply for whole-body energy production. They also have greater activity of rumen epithelial attached oxygen scavenging bacteria that may provide more optimal feed fermentation conditions, which contributes to high feed efficiency.

PREFACE

This thesis is an original product of the author, Rebecca Kong. The experimental protocols reported in Chapters 3 and 4 received approval from the University of Alberta Animal Care and Use Committee for Livestock (Moore-55-2006). All animals were raised in accordance with the Canadian Council of Animal Care guidelines (CCAC, 1993).

DEDICATION

This thesis is dedicated in loving memory of my father, Seu Kong, and my aunt, Milee Lui.

ACKNOWLEDGEMENTS

I would like to express my deepest gratitude to my supervisor, Dr. Leluo Guan, for giving me the opportunity to join her wonderful lab and participate in an exciting project. She provided me with plenty of guidance, patience, and support throughout the program, especially during difficult times. Her trust and great work ethic inspired and motivated me to work hard to achieve my goals. Additionally, being a part of Dr. Guan's lab has provided me with many experiences, great memories and friendships.

I would like to thank Dr. Paul Stothard for being a part of the supervisory committee and Dr. Heather Bruce for being the external examiner. I greatly appreciate their patience, time, and effort.

Also, I would like to thank all the members of Dr. Guan's lab for their friendship, feedback about my research and for answering many of my questions. Thank you Xu Sun for teaching me how to prepare RNA libraries for sequencing. I am really grateful to Yanhong Chen for taking the time to teach me many lab techniques and assisting in the lab work. Also, thank you to Guanxiang Liang and Fuyong Li for their help with analyzing the RNA sequencing data through bioinformatics.

I gratefully acknowledge the funding received for my research from the Alberta Livestock and Meat Agency and Queen Elizabeth II Graduate Scholarship.

Lastly, I want to thank my parents, siblings, and friends for their care and for listening to my stories.

TABLE OF CONTENTS

LIST OF TABLES

LIST OF FIGURES

LIST OF ABBREVIATIONS

ACTB	Actin-beta
ADG	Average daily gain
AE2	Anion exchanger 2
ATP6AP1	ATPase, H+ transporting, lysosomal accessory protein 1
ATP6V0D1	ATPase, H+ transporting, lysosomal 38kDa, V0 subunit D1
B-H	Benjamini Hochberg
BirthWT	Birth weight
CAMs	Cell adhesion molecules
CH_4	Methane
CO_2	Carbon dioxide
COX8A	Cytochrome c oxidase subunit VIIIA
CPM	Count per million reads
CWT	Carcass weight
Ct	Cycle threshold
DAVID	Database for annotation, visualization, and integrated discovery
DDX3Y	DEAD box polypeptide 3, Y-linked
DE	Differentially expressed
DMI	Dry matter intake
DRA	Down-regulated in adenoma
EndWT	End weight
FCR	Feed conversion ratio
FDR	False discovery rate
H_2	Hydrogen
HGS	Hepatocyte growth factor-regulated tyrosine kinase substrate
H-RFI	High residual feed intake
IPA	Ingenuity pathway analysis
KEGG	Kyoto encyclopedia of genes and genomes
L-RFI	Low residual feed intake
MCT1	Monocarboxylate transporter 1

MCT4	Monocarboxylate transporter 4
MEI	Metabolizable energy intake
mtDNA	Mitochondrial DNA
MWT	Metabolic mid-weight
ND1	NADH dehydrogenase subunit 1
nDNA	Nuclear DNA
NPY	Neuropeptide-Y
PANTHER	Protein annotation through evolutionary relationship
PAT1	Putative anion transporter 1
PCA	Principal component analysis
PKM2	Pyruvate kinase m2
POMC	Pro-opiomelanocortin
RFI	Residual feed intake
RNA-seq	RNA-sequencing
SCFAs	Short-chain fatty acids
SLC	Solute carrier
SLC25A39	Solute carrier family 25 member 39
SUZ12	SUZ12 polycomb repressive complex 2 subunit
TCA	Tricarboxylic acid
TECR	Trans-2,3-enoyl-coa reductase
TPI1	Triosephosphate isomerase 1
qPCR	Quantitative real-time polymerase chain reaction
WeanWT	Weaning weight
WGCNA	Weighted gene co-expression network analysis

CHAPTER 1. GENERAL INTRODUCTION

Food security is a major challenge in the future, as the world population is projected to reach 9.6 billion in 2050 (United Nations, 2014). Increased agricultural food production would be needed to feed the growing population, however, the expected increase in urbanization would reduce the amount of land available for agriculture (Tilman et al., 2011; United Nations, 2014). The associated rise in feed prices would be an additional pressure on animal production systems because they will have to produce more than at present with decreased land and increased feed costs (Rosegrant et al., 2008). In beef cattle production, feed accounts for approximately 70% of total costs (Cottle and Kahn, 2014). Therefore, there has been great interest in improving the feed efficiency of cattle. Feed efficiency is defined as how well an animal converts feed into energy for use in growth and maintenance requirements. Selecting for high feed efficiency would not only reduce feed cost, but it would also decrease the environmental impact of beef cattle production. For example, feed efficient cattle are known to produce around 28% less methane (CH_4) and 15% less manure than feed inefficient cattle (Okine et al., 2001; Nkrumah et al., 2006). A decrease in CH_4 production from ruminants such as cattle would help reduce global CH_4 emissions as enteric CH_4, largely from ruminants, contributes to about 17% of global CH_4 emissions (Knapp et al., 2014). Additionally, a 10% improvement in feed efficiency would result in a 43% increase in profit, whereas a 10% improvement in rate of gain increased profits by only 18% (Fox et al., 2001). Therefore, it would be beneficial to improve feed efficiency for increased profitability, sustainable beef production, and minimization of the environmental footprint of production.

The following literature review aims to describe the most commonly used feed efficiency selection measures and the many factors that contribute to variation in beef cattle feed efficiency.

Emphasis will be given to describe the rumen microbial ecology of beef cattle and their effect on feed efficiency as well as elaborate on the host-microbial symbiotic relationship. The literature review will also provide details about the structure of the rumen epithelium and its role in the absorption and metabolism of energetic substrates for the host to utilize as energy. Additionally, the recent advances in technology used to quantify gene expression will be discussed.

CHAPTER 2. LITERATURE REVIEW

2.1 Measures of feed efficiency

2.1.1 Feed conversion ratio

The feed conversion ratio (FCR) is the ratio of feed intake to rate of gain and is the most commonly used measure of feed efficiency in beef operations (Arthur et al., 2001). A low FCR is more desirable because it indicates that an individual requires less feed per unit of gain. However, FCR is a gross measure of feed efficiency that does not account for the maintenance requirements of body size. FCR is therefore not considered a good indicator of feed efficiency since dietary energy is not partitioned between growth and maintenance requirements. Also, FCR is not an optimal trait for genetic selection due to its negative correlation with growth rate (Arthur et al., 2001). Selection for low FCR may therefore result in larger, faster growing cattle (Herd and Bishop, 2000) that would have greater maintenance and feed requirements, which consequently lead to higher feed cost.

2.1.2 Residual feed intake

Unlike FCR, residual feed intake (RFI) is a net feed efficiency measure that accounts for the maintenance requirements of an animal based on its body size (Arthur and Herd, 2008). RFI is the difference between actual feed intake and the expected feed intake based on maintenance and growth requirements. Expected feed intake is calculated by a regression of dry matter intake on the growth traits, average daily gain (ADG) and metabolic mid-weight (MWT) (Basarab et al., 2003). A low (negative) RFI (L-RFI) indicates that an individual consumes less feed than expected and is feed efficient. However, an animal that consumes more feed than expected has a high (positive) RFI (H-RFI) and is considered feed inefficient. RFI is not correlated to the two

component traits (MWT and ADG) used to calculate it (Herd and Bishop, 2000; Arthur et al., 2001), which suggests that selection for L-RFI (feed efficient) cattle would not influence growth traits and negatively impact feed cost. The independence of RFI from growth traits also allows for the comparison of feed efficiency between animals differing in production (Arthur and Herd, 2008). Over a 120-day period, L-RFI steers would lead to savings of $45.60 per head due to 3.77 kg lower feed intake per day (Basarab et al., 2003). It is uncertain whether selection for RFI would affect economically important meat quality traits. Studies have shown that selection for RFI would not impact meat quality traits such as the yield grade, marbling score, and tenderness (Baker et al., 2006; Castro Bulle et al., 2007; Perkins et al., 2014). However, others have found that selection for L-RFI cattle may negatively affect meat tenderness (McDonagh et al., 2001).

Measurement of RFI was highly labor intensive until the GrowSafe automated feeding system (GrowSafe Systems Ltd., Airdrie, Alberta, Canada) was developed. GrowSafe allowed for simplified measurement of feed intake by automatic recordings through radio frequency ID tags on animals, wireless transmission of data, and software for data analyses (Basarab et al., 2002). However, RFI measurement has not been highly adopted because it is expensive ($150-$188 per animal; Basarab et al., 2002) and time consuming (~70-84 days; Archer and Bergh, 2000). Thus there has been growing interest in developing a genetic selection tool for the improvement of feed efficiency. RFI is an ideal trait for genetic selection due to its moderate heritability (0.28 to 0.45) (Koch, 1963; Arthur et al., 2001; Crowley et al., 2010) and independence from growth traits (Herd and Bishop, 2000; Arthur et al., 2001).

2.2 Factors contributing to variation in feed efficiency

Differences in many physiological processes in cattle contribute to variation in feed efficiency. Physiological processes that have been found to impact RFI include those associated

with feed intake, digestion, metabolism, activity, and stress (Richardson and Herd, 2004; Herd and Arthur, 2009). Richardson and Herd (2004) have predicted the contribution of some of the physiological mechanisms to differences in beef cattle RFI. They indicated that feeding patterns contributed to 2% of the variation in RFI, while digestibility contributed 10%, body composition 5%, activity 10%, and heat increment of feed fermentation 9% to the variation in RFI. Additionally, a large proportion of the variation in RFI (37%) was attributed to differences in protein turnover, tissue metabolism, and stress. There was also 27% of the variation due to unidentified factors.

The feeding behavior of beef cattle differs between feed efficient (L-RFI) and inefficient (H-RFI) individuals. H-RFI steers have been associated with a longer feeding duration, more feeding sessions, and a more variable feeding pattern throughout the day than L-RFI steers (Nkrumah et al., 2006; Golden et al., 2008). The feeding behavior of inefficient animals may contribute to greater feed intake and energy expenditure. H-RFI animals have increased energy expenditure through increased feeding and locomotion activity as well as an increased heat increment of feeding (Richardson et al., 1999; Nkrumah et al., 2006). The heat increment of feeding was reported to be 32.6% higher in H-RFI steers compared to L-RFI individuals (Nkrumah et al., 2006). When body composition was compared between RFI groups, there was increased fat and reduced protein deposition in H-RFI cattle (Richardson et al., 2001; Basarab et al., 2003). Fat is more energetically expensive to deposit than protein (Owens et al., 1995). Additionally, when tissue metabolism and stress was examined, inefficient animals were most susceptible to stress (Richardson et al., 2002) and had the greatest protein turnover in the skeletal muscle (McDonaugh et al., 2001). Increased fat deposition, stress, and protein turnover contributes to increased energy expenditure in H-RFI animals, which indicates inefficiency in energy utilization. Also, feed digestibility tends to be negatively correlated with RFI (r=-0.33;

$p<0.10$) (Nkrumah et al., 2006). Increased feed digestibility in L-RFI cattle contributes to reduced feed intake and increased feed efficiency as additional energetic substrates are derived from feed for utilization. Overall, feed efficient (L-RFI) cattle consume less feed than inefficient (H-RFI) cattle due to factors such as reduced energy expenditure and increased feed digestibility.

Physiological processes are influenced by both genetic and environmental factors. Diet is an environmental factor that could impact the feed efficiency of cattle. For example, a change from a low-energy-density to high-energy-density diet has been associated with RFI re-ranking in beef steers (Durunna et al., 2011). RFI re-ranking of an individual based on diet may be attributed to the efficiency of their rumen microorganisms to degrade and ferment different feedstuffs to supply energetic substrates to the host. Further information about how the rumen microorganisms are associated with feed efficiency will be provided later in this review. The molecular mechanisms underlying many of the host physiological processes that contribute to variation in feed efficiency are largely unknown. Because numerous processes influence RFI, many genes are likely involved in affecting feed efficiency. Therefore, there has been difficulty in marker-assisted selection for RFI. Perkins and colleagues (2014) have attempted to identify and describe the molecular mechanisms underlying feed intake in beef steers divergent in RFI. Using quantitative real-time polymerase chain reaction (qPCR), they determined the expression of genes within the hypothalamus and adipose tissue that have known roles in affecting feed intake. They found that the hypothalamus of L-RFI steers had reduced expression of neuropeptide-Y (*NPY*) and increased expression of pro-opiomelanocortin (*POMC*). NPY stimulates feeding behavior (orexigenic), while POMC is known to inhibit feeding behavior (anorexigenic). Therefore, L-RFI steers may have lower feed intake due to decreased feeding behavior caused by decreased expression of an orexigenic gene (*NPY*) and increased expression of an anorexigenic gene (*POMC*). Additionally, leptin expression in the adipose tissue was

greatest in L-RFI animals, which may also decrease feed intake through the stimulation of satiety. Studies have also examined the molecular mechanisms involved in metabolism between cattle differing in RFI (Chen et al., 2011). The liver transcriptomes of cattle were examined using a microarray containing 24,000 probes (Chen et al., 2011). There were 161 differentially expressed (DE) genes between the livers of L- and H- RFI cattle. Functional analysis showed that the most significantly enriched function was cellular growth and proliferation, which contained 19 DE genes that were up-regulated in L-RFI animals. The L-RFI individuals may have increased cellular growth and proliferation due to efficient energy generation from energetic substrates obtained from feed. However, all analyses derived from gene expression data require validation through additional experiments. Further work needs be conducted to identify and understand all the molecular mechanisms that affect RFI and verify the role of candidate genes within these mechanisms.

2.3 Advances in technology used to quantify gene expression

Transcripts that are generated from the transcription of genes are quantified as an indication of gene expression. The qPCR technique has been commonly used to quantify gene expression by targeting specific transcripts using primers designed based on known sequences. Primers anneal to their target transcript and the target is amplified through synthesis, which is detected by fluorescence. The quantity of the amplification product and therefore, the relative quantity of the target transcript, is measured through the intensity of fluorescence. A drawback of qPCR is that it is a low-throughput method that measures the expression of a limited number of genes within a run. Additionally, qPCR can only measure the expression of genes that have known sequences. The development of microarray technology provided a high-throughput method to measure the expression of many genes. A microarray contains pre-designed

oligonucleotide probes that target specific gene transcripts. The abundance of a specific gene transcript is quantified through the intensity of fluorescence emitted by the hybridization of transcripts to their corresponding probe. Since the microarray detects gene expression based on hybridization of transcripts to probes of known sequence, novel gene sequences cannot be detected. The recent development of high-throughput RNA-sequencing (RNA-seq) technology has allowed us to quantify whole gene expression profiles (transcriptome) within organisms. Using RNA-seq technology, all transcripts in a sample are sequenced by synthesis and bioinformatics software is used to align transcripts to a reference genome in order to quantify the expression of known and novel genes.

2.4 The rumen of ruminant animals

Ruminant animals such as cattle have four stomach compartments (rumen, reticulum, omasum, abomasum) involved in the digestion and fermentation of feed. The rumen is the first and the largest of the stomach compartments with a capacity of 68 to 86 litres in beef cattle. It is the main site of feed fermentation by a large and diverse community of symbiotic microorganisms, which is why ruminant animals are categorized as foregut fermenters.

2.4.1 The rumen microbial community

The rumen microbial community is comprised of bacteria (10^{10}-10^{11}/mL), protozoa (10^{5}-10^{6}/mL), fungi (10^{2}-10^{3}/mL), archaea (10^{7}/mL), and bacteriophage (10^{7}-10^{9}/mL) (Fonty et al., 1987; Klieve and Swain, 1993; Hobson and Stewart, 1997; Singh et al., 2013). There are three different populations of microorganisms such as those associated with rumen fluid, particles or epithelium (McCowan et al., 1978; Olubobokun and Craig, 1990). Approximately 70-80% of the rumen microbes are associated with feed particles, 20-30% with fluid, and 1-2% with the epithelium (Craig et al., 1987).

2.4.2 Host symbiotic relationship with ruminal microorganisms

Rumen microorganisms have a symbiotic relationship with the ruminant host. They provide many benefits such as feed degradation and fermentation, microbial protein and vitamin production. In return, the host provides the necessary conditions for the microbes to survive.

2.4.2.1 Benefits of rumen microorganisms to the host

2.4.2.1.1 Microbial feed degradation

Ruminal bacteria, protozoa and fungi are synergistically involved in the degradation of the structural polysaccharides, non-structural polysaccharides, and protein in plant material to simple monosaccharides and amino acids (Zhang et al., 2007). The rumen microorganisms are necessary to the ruminant host because vertebrates lack the enzymes needed to hydrolyze structural polysaccharides of the plant cell wall such as cellulose, hemicellulose and pectin (Sues, 2005). Many of the rumen bacterial species possess hydrolytic enzymes that breakdown the linkages within the complex carbohydrates (Table 2.1) (Cheng et al., 1984; Sues, 2005). Fungi play an important role in the enzymatic degradation of lignin in the plant cell wall, which allows bacteria easier access to substrates (Akin and Borneman, 1990).

Table 2.1. Major rumen bacterial species that degrade structural polysaccharides in the plant cell wall (adapted from Cheng et al., 1984).

Cell wall structural polysaccharide	Bacterial species
Cellulose	*Bacteroides succinogenes* *Ruminococcus flavefaciens* *Ruminococcus albus* *Butyrivibrio fibrisolvens* *Cillobacterium cellulosolvens* *Clostridium lachheadii* *Cellulomonas fimi* *Eubacterium* spp.
Hemicellulose	*Butyrivibrio fibrisolvens* *Ruminococcus flavefaciens* *Ruminococcus albus* *Bacteroides ruminicola*
Pectin	All the cellulolytic and hemicellulolytic species plus: *Lachnospira multiparus* *Streptococcus bovis* *Succinovibrio dextrinosolvens*

2.4.2.1.2 Carbohydrate fermentation by ruminal microbes

Rumen bacteria are responsible for the fermentation of the simple carbohydrates (hexoses and pentoses) generated from the degradation of structural polysaccharides (cellulose, hemicellulose and pectin) and non-structural polysaccharides (starch) (Figure 2.1) (Dijkstra et al., 2005; Hvelplund et al., 2009). Through the Embden-Myerhoff fermentation pathway, simple carbohydrates are converted into short-chain fatty acids (SCFAs), mainly acetate, propionate, and butyrate (Figure 2.1) (Dijkstra et al., 2005). The fermentation of carbohydrates yields large amounts of energy for microbial growth. Also, the SCFAs are highly important to the host because they can contribute up to 70% of the animal's energy requirement (Bergman, 1990). Methanogenic archaea utilize the waste products of fermentation, such as formate, hydrogen (H_2), and carbon dioxide (CO_2) to generate methane (CH_4) (Figure 2.1) (Dijkstra et al., 2005).

The removal of H_2 is important in maintaining optimal conditions for fermentation since H_2 is known to inhibit the complete oxidation of substrates.

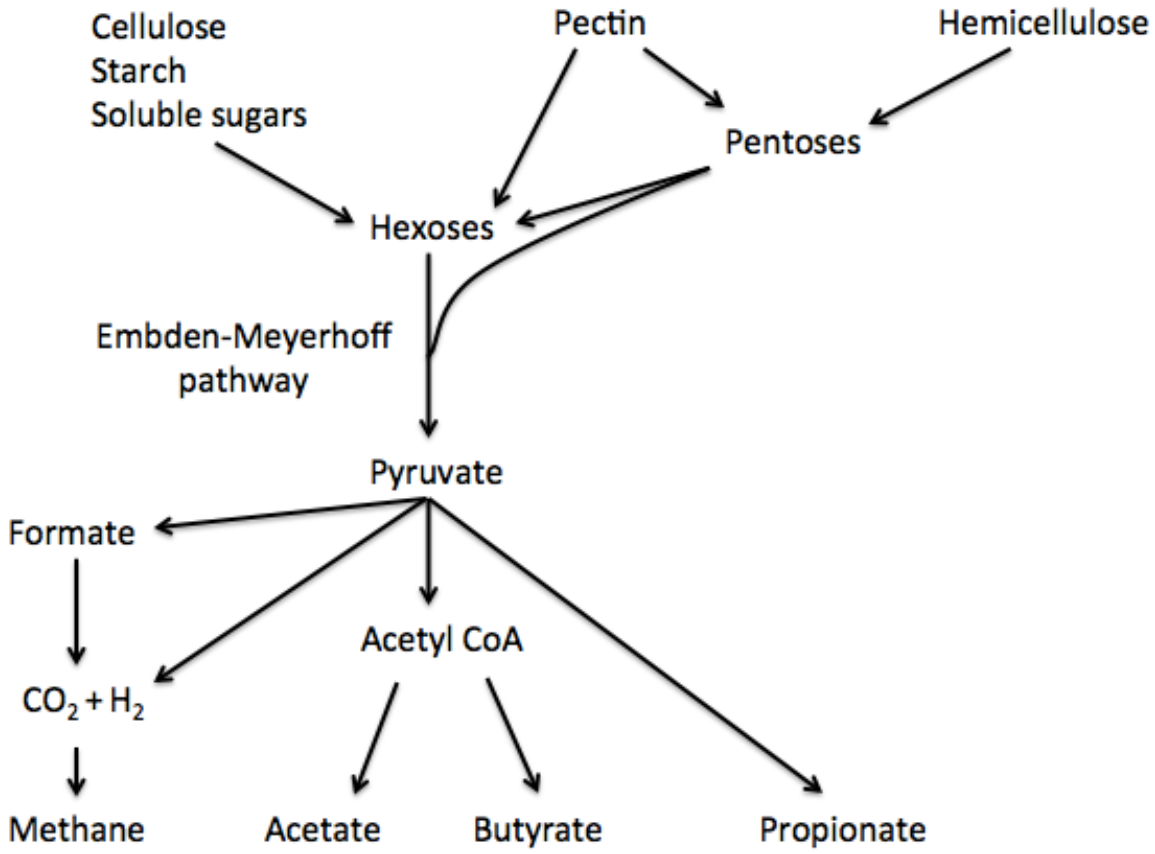

Figure 2.1 Pathway of carbohydrate metabolism in the rumen (adapted from Dijkstra et al., 2005).

2.4.2.1.3 Microbial protein and vitamins

Ruminal microbes require nitrogen sources to generate microbial protein for growth (Argyle and Baldwin, 1989). They digest dietary protein to obtain amino acids, which are used to synthesize microbial protein directly or fermented for energy (Broderick and Craig, 1989; Atasoglu et al., 1998). Ammonia is another important nitrogen source for microbial protein synthesis, which is produced as a byproduct of fermentation and also obtained through the

hydrolysis of urea (Obara and Shimbayashi, 1980; Broderick and Craig, 1989). The growth of ruminal microbes is highly important to host nutrition because the microbial biomass entering the small intestine is the largest source of protein for ruminants (McCarthy et al., 1988). Additionally, ruminal microbes synthesize sufficient B-vitamins and vitamin K to satisfy the host requirements (Schwab et al., 2006).

2.4.2.1.4 Additional benefits of rumen epithelial-attached microbes

Surface epithelial cells are often sloughed from the stratified squamous epithelium of the rumen (Goodlad, 1981). It has been suggested that the bacterial population attached to the epithelium are highly proteolytic and assist the host in the removal of dead epithelial cells (Dinsdale et al., 1980; McCowan et al., 1978). The bacteria infiltrate and digest the dead cells, thereby recycling the protein for the host (Dinsdale et al., 1980). During the removal of surface cells from the epithelium, the bacteria quickly colonize the new underlying epithelial layer (McCowan et al., 1978). This is important to the host because the microbial biofilm on the epithelium may act as a barrier against fermentation products that could harm the mucosa. Additionally, there are anti-oxidant producing bacteria on the epithelium that protect cells from oxidative stress through the reduction of reactive oxygen species (Holovska et al., 2002). The removal of reactive oxygen species by epithelial-attached microbes helps prevent damage to cell membranes.

Many of the facultative anaerobes that adhere to the epithelium are capable of oxygen scavenging (Cheng et al., 1979). They maintain the anaerobic condition of the rumen by metabolizing the oxygen that diffuses from the epithelial tissue (Cheng et al., 1979). Maintaining the anaerobic condition protects the obligate anaerobes and therefore ensures effective feed

fermentation (Cheng et al., 1979). This benefits both the host and ruminal microbes because the fermentation process provides them with nutrients and energy.

The facultative anaerobes attached to the epithelium are also largely responsible for hydrolyzing the urea that diffuses across the tissue (Cheng et al., 1979). Urease activity is beneficial since the hydrolysis of urea provides ammonia to microbes for protein synthesis (Laukova and Koniarova, 1995; Pilgrim et al., 1970). Studies have found that when rumen ammonia concentration was low, there was increased urease activity to increase the ammonia concentration (Cheng and Wallace, 1979).

2.4.2.2 Host benefits to ruminal microorganisms

The ruminant host provides benefits to the rumen microbiota. For example, the rumen has an anaerobic environment essential to the survival of microorganisms that are sensitive to oxygen (Van Soest, 1994). The host maintains the temperature of the rumen at around 39°C, which is optimal for fermentation and for the growth of many ruminal microbes (Lowe et al., 1987; Bhatta et al., 2006; Wahrmund et al., 2012). Studies have found that an increase in temperature from 39°C to 41°C reduced the amount of feed degradation by microorganisms (Bhatta et al., 2006). Additionally, the host supplies the substrates that are needed by the microorganisms to obtain nutrients for activity and growth.

2.5 Role of rumen microorganisms in feed efficiency

There tends to be increased feed digestibility within the rumen of feed efficient cattle, which may be attributed to efficient feed digestion and fermentation by rumen microorganisms (Nkrumah et al., 2006). Indeed, the rumen fluid of L-RFI animals tends to have a greater concentration of total SCFAs ($p=0.059$) and significantly greater concentration of butyrate and valerate ($p<0.01$) than the rumen fluid of H-RFI animals (Guan et al., 2008). Studies have

identified an association between the rumen microbial profile, fermentation parameters, and feed efficiency (Guan et al., 2008; Hernandez-Sanabria et al., 2010; Hernandez-Sanabria et al., 2012). Clustering analysis of bacterial profiles in the ruminal fluid and solid showed that the profiles of L-RFI steers clustered together and away from H-RFI profiles (Guan et al., 2008). Also, the L-RFI bacterial profiles were more similar to each other (91% similarity) than the H-RFI profiles (71% similarity). This suggests that the efficient (L-RFI) animals contain a specific consortium of bacteria that may be most efficient for feed digestion and fermentation. The abundance of particular bacterial phylotypes may also contribute to differences in RFI (Hernandez-Sanabria et al., 2012). For example, there was a positive correlation of *Eubacterium* sp. with RFI under a high-energy-density diet.

Efficient cattle may have lowered CH_4 production due to differences in the methanogen population in the rumen. The total abundance of methanogens in ruminal fluid has been found to not differ between RFI groups (Zhou et al., 2009, Zhou et al., 2010). Specific methanogen phylotypes, however, are associated with differences in RFI. For instance, H-RFI steers had greater abundance of *Methanosphaera stadtmanae* and *Methanobrevibacter* sp. strain AbM4 as measured by sequencing of the 16S rRNA gene (Zhou et al., 2009).

2.6 Rumen epithelium structure and function

2.6.1 Rumen epithelial strata and functions

The rumen tissue has a stratified squamous epithelium composed of four strata (Graham and Simmons, 2005). From the lumen to the basal lamina, these strata are the stratum corneum, stratum granulosum, stratum spinosum, and stratum basale. Graham and Simmons (2005) showed that the stratum corneum is highly keratinized and acts as a physical barrier against the contents of the rumen. Within the stratum granulosum there was an abundance of junctional

complexes, which suggests it has a role as a permeability barrier. For example, there was high expression in the stratum granulosum of a gap junction component (connexin 43) and tight-junction molecules (claudin-1 and zonula occludens-1). The high density of mitochondria in the stratum spinosum and basale, indicate these layers have high metabolic function.

2.6.2 Short-chain fatty acid absorption from the rumen

A majority of the SCFAs produced from microbial fermentation are absorbed from the rumen (Peters et al., 1990; Peters et al., 1992). SCFA absorption occurs through the mechanisms of simple diffusion and protein-mediated transport (López et al., 2003; Aschenbach et al., 2009). The simple diffusion of SCFAs arises due to the generation of a concentration gradient between the rumen content, epithelial cell cytosol, and portal circulation (López et al., 2003). Additionally, the decrease in pH associated with high SCFA concentration in the rumen results in enhanced absorption (Dijkstra et al., 1993; López et al., 2003). Rumen epithelial cell metabolism of SCFAs may also contribute to maintaining the concentration gradient for simple diffusion. For example, the fractional absorption rate was found to be greatest for butyrate, then propionate and acetate (Dijkstra et al., 1993), which correspond to the amount of their metabolism in the epithelium (Kristensen et al., 1996; Sehested et al., 1999; Kristensen et al., 2000a,b). Protein-mediated absorption of SCFAs occurs through bicarbonate-dependent and bicarbonate-independent mechanisms (Aschenbach et al., 2009). The currently known or candidate SCFA transporters belong to solute carrier (SLC) families such as SLC4A, SLC16A (monocarboxylate transporters), SLC21A, SLC22A, or SLC26A (Aschenbach et al., 2009). Known SCFA transporters include putative anion transporter 1 (PAT1, SLC26A6), down-regulated in adenoma (DRA, SLC26A3), anion exchanger 2 (AE2, SLC4A2), monocarboxylate transporter 1 (MCT1, SLC16A1), and monocarboxylate transporter 4 (MCT4, SLC16A3). The

transporters PAT1, DRA, and AE2 operate through exchange of bicarbonate for SCFA (Mount and Romero, 2004; Romero et al., 2004). Monocarboxylate transporters function in a bicarbonate-dependent manner (Hadjiagapiou et al., 2000), as well as through co-transport of proton and SCFA (Becker and Deitmer, 2008). Studies have found increased rumen epithelial expression of *PAT1*, *DRA*, *AE2*, *MCT1*, and *MCT4* when SCFA concentration increased (Yan et al., 2014). Also, an increase in bicarbonate-dependent SCFA absorption was observed with increasing SCFA concentration and decreasing ruminal pH (Aschenbach et al., 2009).

2.6.3 Short-chain fatty acid metabolism within the rumen epithelium

The rumen epithelium is capable of metabolizing SCFAs. Approximately 68-95% of absorbed butyrate, 15-78% of propionate, and 26-55% of the acetate is metabolized in the rumen epithelium (Kristensen et al., 1996; Sehested et al., 1999; Kristensen et al., 2000a,b). SCFAs are converted to acetyl-CoA through the process of β-oxidation to enter into energy generating pathways, such as the tricarboxylic acid cycle and electron transport chain (Van Soest, 1994). Also, ketogenic enzymes present in the mitochondria convert SCFAs to ketone bodies (beta-hydroxybutyrate and acetoacetate), which are an important circulating source of energy (Lane et al., 2002). Ketone bodies are primarily produced in the liver and rumen. Therefore, the extensive metabolism of SCFAs in the epithelium indicates that the rumen epithelium plays an important role in whole-body energy generation.

2.7 Summary of literature review in relation to research objectives and hypotheses

The molecular mechanisms underlying biological processes that contribute to variation in feed efficiency have yet to be fully elucidated. Studies have examined gene expression within tissues such as the hypothalamus, adipose, and liver in beef cattle divergent in RFI (Chen et al., 2011; Perkins et al., 2014). However, the role of the rumen epithelium in feed efficiency has not

yet been studied. The objective of the first study was to examine the contribution of the rumen epithelium to differences in feed efficiency. It was aimed to analyze the gene expression differences between the rumen epithelial tissues of feed efficient (L-RFI) and inefficient (H-RFI) beef cattle using RNA-seq. The hypothesis was that the rumen epithelium of feed efficient individuals would have greater expression of genes involved in regulating the absorption and metabolism of energetic substrates, such as SCFAs. Additionally, it is unknown how rumen epithelial attached microbes influence feed efficiency as studies have only examined the rumen content microorganisms (Guan et al., 2008; Zhou et al., 2009; Hernandez-Sanabria et al., 2010; Zhou et al., 2010; Hernandez-Sanabria et al., 2012). The second study, therefore, assessed the differences in the activity of the rumen epithelial attached bacteria and archaea of beef cattle differing in RFI. It was predicted there would be lower activity of CH_4-producing archaea on the L-RFI epithelium since feed efficient animals produce less CH_4. Also, it was hypothesized that L-RFI animals would have greater activity of ureolytic and oxygen scavenging bacteria that would provide more ammonia for microbial protein synthesis and better fermentation conditions, respectively.

CHAPTER 3. TRANSCRIPTOME PROFILING OF THE RUMEN EPITHELIUM OF BEEF CATTLE DIFFERING IN RESIDUAL FEED INTAKE

3.0 Introduction

Feed is one of the major costs in beef cattle production, accounting for approximately 70% of total expenditures (Cottle and Kahn, 2014). As feed price continues to rise due to factors such as human population growth and decreasing amount of arable land (Alston and Pardey, 2014), beef cattle feed efficiency has become an increasingly important contributor to reducing the cost of production. Recent efforts in the selection of feed efficient cattle have been focused on residual feed intake (RFI), a measure of feed efficiency that is independent of growth and body weight (Arthur et al., 2001). The RFI of an individual is calculated as the difference between actual feed intake and expected feed intake based on maintenance and growth requirements (Basarab et al., 2003). Animals with low (negative) RFI (L-RFI) are considered feed efficient because they consume less feed than expected whereas animals with high (positive) RFI (H-RFI) are feed inefficient due to consuming more feed than expected. Selection for L-RFI animals would not only reduce cost of production, but also decrease the environmental footprint because they produce 28 and 15% less methane (Nkrumah et al., 2006) and manure (Okine et al., 2001), respectively, than H-RFI animals.

Variation in RFI may be due to differences in many biological processes that are influenced by genetic and environmental factors. Physiological processes that have been found to contribute to variation in RFI include those associated with feed intake, digestion, metabolism, activity, and stress (Richardson and Herd, 2004; Herd and Arthur, 2009). Genetic selection and improvement of RFI is possible since RFI is a moderately heritable trait (0.28 to 0.45) (Koch, 1963; Arthur et al., 2001; Crowley et al., 2010), however, the molecular mechanisms underlying RFI are largely

unknown. Because variation in RFI is due to differences in many processes, multiple genes from various pathways are likely involved (Chen et al., 2011; Karisa et al., 2013; Perkins et al., 2014). Discovering differences at the molecular level may potentially lead to identification of biomarkers for use in the selection of L-RFI (feed efficient) animals.

In ruminant animals, such as cattle, the rumen may play an important role in feed efficiency. It is the main site of microbial feed digestion and fermentation that produces short-chain fatty acids (SCFAs), which are a major energy source for cattle accounting for up to 80% of total energy requirements (Wolin, 1979; Bergman, 1990). SCFAs are mainly absorbed from the rumen (López et al., 2003) and metabolized within the rumen epithelium, liver and peripheral tissues to generate energy for use in maintenance, growth and activity (Ash and Baird, 1973; Nayananjalie et al., 2015). Studies have indicated that SCFAs are absorbed by both simple diffusion (López et al., 2003) and protein-mediated transport through bicarbonate -dependent and -independent mechanisms (Aschenbach et al., 2009). Moreover, ketogenic enzymes within the mitochondria of the rumen epithelium play a crucial role in the metabolism of SCFAs, to produce ketone bodies that are an important circulating source of energy throughout the body (Robinson and Williamson, 1980; Leighton et al., 1983).

Differences in the ability of the rumen epithelium to absorb and metabolize SCFAs may be associated with variation in feed efficiency. Therefore, the objective of this study was to investigate differences in gene expression between the rumen epithelial tissues of feed efficient and inefficient beef cattle using RNA-sequencing (RNA-seq) technology and bioinformatics. We hypothesized that the rumen epithelium of L-RFI (efficient) animals would have greater expression of genes involved in absorption and metabolism of energetic substrates such as SCFAs.

3.1 Materials and Methods

3.1.1 Animals and rumen tissue collection

Hereford x Aberdeen Angus hybrid steers (n=175) were born in the spring of 2006 and raised at the University of Alberta Roy Berg Kinsella Research Station (Alberta, Canada) in accordance with the Canadian Council of Animal Care guidelines (CCAC, 1993). The University of Alberta Animal Care and Use Committee for Livestock approved the experimental protocols (Moore-55-2006).

Steers were under feedlot conditions while feed intake data was collected using the GrowSafe automated feeding system (GrowSafe Systems Ltd., Airdrie, Alberta, Canada). The finishing diet was fed for 90 days and was composed of 56.7% barley, 28.3% oats, 10% alfalfa pellets, and 5% feedlot supplement (32% crude protein beef supplement containing Rumensin (400 mg/kg) and 1.5% canola oil). After slaughter, a 4-cm^2 piece of rumen tissue was obtained from the central region of the ventral sac and rinsed with sterilized PBS buffer (pH = 6.8) before being placed in a 50 mL tube containing RNAlater solution (Invitrogen, Carlsbad, CA). The samples were then stored at -80°C until further processing.

RFI values were calculated as described by Nkrumah et al. (2006) and animals were classified as L-RFI (feed efficient; RFI < -0.5), medium RFI (M-RFI; -0.5 ≤ RFI ≤ 0.5), or H-RFI (feed inefficient; RFI > 0.5). The rumen epithelium from the most extreme L-RFI (n=9; RFI = -1.4 to -2.33 kg/day) and H-RFI (n=9; RFI = 1.32 to 3.23 kg/day) steers were selected and used for RNA-seq and transcriptome analysis.

3.1.2 RNA extraction and sequencing

After thawing, rumen tissue was placed on a petri dish and papillae (~80 mg) were obtained using sterile scissors and scalpels. The total RNA was extracted from the papillae using

mirVana kit (Ambion, Austin, TX) according to the manufacturer's instructions. RNA integrity of the total RNA samples was assessed using the Agilent 2100 Bioanalyzer (Agilent Technologies, Santa Clara, CA) and Nanodrop 2000c spectrophotometer (Thermo Scientific, Wilmington, DE) was used to measure the concentration and purity. Only samples with RNA integrity greater than 7 were subjected to RNA-seq library construction.

For each of the 18 samples, a cDNA library was generated from 100 ng of total RNA following the protocol of the TruSeq RNA Sample Preparation v2 kit (Illumina, San Diego, CA). First, total RNA was fragmented and cDNA was synthesized through reverse transcription. The resulting double-stranded cDNA was then subjected to end repair and 3'-end adenylation before ligation of index adapters. Libraries were amplified by 15 cycles of PCR, then validated with the Agilent 2200 TapeStation (Agilent Technologies) and quantified with a Qubit fluorometer using a Qubit dsDNA HS Assay Kit (Invitrogen, Carlsbad, CA). The individual indexed libraries were then pooled and sequenced in five lanes on the Illumina HiSeq 2000 system at the McGill University and Genome Quebec Innovation Centre (Quebec, Canada) to obtain high-quality, 100-bp paired-end reads (Average Phred quality score $\geq$ 33). The raw sequencing data have been deposited at publicly available NCBI's Gene Expression Omnibus Database (http://www.ncbi.nlm.nih.gov/geo/). The data are accessible through GEO Series accession number GSE74394 (http://www.ncbi.nlm.nih.gov/geo/query/acc.cgi?acc=GSE74394).

3.1.3 Transcriptome mapping

We used the software package TopHat2 (v2.0.9) (Kim et al., 2013) with Bowtie2 (v2.1.0) (Langmead and Salzberg, 2012) to align the high-quality RNA-seq reads to the bovine reference genome, UMD3.1 (Ensembl v83.31). Samtools (v1.1) (Li et al., 2009) was used to sort the BAM alignment files that were generated from TopHat2 by name and these sorted BAM files were

converted to SAM files for input to HTSeq-count (v0.6.1) (Anders et al., 2015), which is a software tool that counts the number of reads per gene using the Ensembl (v83.31) bovine gene annotation.

3.1.4 Differential gene expression and principal component analysis

Differential gene expression analysis was performed using the Bioconductor (v3.0; Gentleman et al., 2004) package DESeq2 (v1.6.2; Love et al., 2014) in the R statistical software program (v3.1.2; R Core Team, 2014). Firstly, DESeq2 normalized gene count data using the relative log expression method based on "size factors" to account for RNA-seq library size differences and dispersion estimates were calculated. Then, pairwise comparison of expression was made between the L-RFI and H-RFI group for every gene based on a negative binomial model. Fold changes were obtained along with their associated p-values. The Benjamini Hochberg method (B-H) was used to control the false discovery rate (FDR) by adjusting p-values to correct for multiple testing. A gene was defined as differentially expressed (DE) between the L-RFI and H-RFI group if it had a B-H adjusted p-value (FDR) less than 0.05.

DESeq2 was also used for Principal Component Analysis (PCA) to cluster samples based on gene expression data. Firstly, count data was normalized based on library size and rlog transformed. The top 500 genes with the most variance (i.e. Largest standard deviations) were compared between samples to calculate principal components in order to view clustering in two dimensions.

3.1.5 Weighted Gene Co-expression Network Analysis (WGCNA)

The WGCNA R software package (v1.41.1; Langfelder and Horvath, 2008) was used to identify modules containing genes that are co-expressed and correlated with the RFI trait. Gene expression data was firstly filtered by keeping genes with at least one read in 50% of the

samples, then normalized by count per million reads (CPM) and Log2 transformed (Log2(CPM+1)). Removal of the very lowly expressed genes resulted in 14,916 genes for input to WGCNA. Unsigned, weighted correlation network construction and module detection was performed using the automatic one-step function, blockwiseModules. The resulting gene modules were assigned color names by the software and Module-Trait relationships were calculated by Pearson correlation. Modules with statistically significant ($p<0.05$) correlations were selected for downstream analysis as potential biologically interesting modules associated with the RFI trait. Additionally, a hierarchical clustering dendrogram of samples and trait heatmap was created using unfiltered, Log2CPM data. Sample clustering was based on Euclidean distance and the traits used in the heatmap were residual feed intake (RFI), dry matter intake (DMI), metabolizable energy intake (MEI), birth weight (BirthWT), weaning weight (WeanWT), metabolic mid-weight (MWT), end weight (EndWT), carcass weight (CWT), and average daily gain (ADG).

3.1.6 Functional gene annotation

Ensembl gene ID lists were converted to gene names and symbols using the Database for Annotation, Visualization, and Integrated Discovery (DAVID; Huang et al., 2009a,b) and the R/Bioconductor package, biomaRt (v2.22.0; Durinck et al., 2009). DAVID and Ingenuity Pathway Analysis (IPA; QIAGEN Redwood City, www.qiagen.com/ingenuity) were used for functional annotation of DE genes and WGCNA gene modules. In DAVID, we examined genes for enrichment in functional categories such as SP_PIR_Keywords and Kyoto Encyclopedia of Genes and Genomes (KEGG) pathways (Kanehisa and Goto, 2000; Kanehisa et al., 2014). To correct for multiple testing in DAVID, p-values were adjusted using B-H correction. Biological terms were considered significant if the adjusted p-value was less than 0.05. The genes input to

IPA were compared to the manually curated Ingenuity knowledge base to find significantly enriched canonical pathways, and cellular and molecular processes. Statistical significance ($p<0.05$) was calculated using the right-tailed Fischer's Exact Test.

The identified core transcripts (i.e. genes with at least one read in every sample) were input to the Protein Annotation Through Evolutionary Relationship (PANTHER; Mi et al., 2013) gene list analysis tool to determine the core functions of the rumen epithelium. Functional classification of genes in categories such as molecular function and biological process was based on Gene Ontology (GO) annotations.

3.1.7 Quantitative real-time PCR (qPCR) validation of DE genes

To validate the identified DE genes from RNA-seq, total RNA was extracted from rumen papillae of 30 L-RFI samples (RFI = -0.51 to -2.33 kg/day) and 27 H-RFI samples (RFI = 0.66 to 3.23 kg/day), respectively. Primers targeting five selected DE genes including Trans-2,3-Enoyl-CoA Reductase (*TECR*), Cytochrome C Oxidase Subunit VIIIA (*COX8A*), Solute Carrier Family 25 Member 39 (*SLC25A39*), Pyruvate Kinase M2 (*PKM2*) and Triosephosphate Isomerase 1 (*TPI1*) were designed using Primer-BLAST (NCBI, Bethesda, MD), Primer Express software (Applied Biosystems, Foster City, CA) or obtained through literatures. The specificity of primers was checked with BLAST (NCBI) and the UCSC In-Silico PCR program (Kuhn et al., 2012). Table 3.1 lists the housekeeping gene (endogenous control) and the five DE genes selected for qPCR validation along with their GenBank accession number, primer sequences, product length and functional pathway.

All samples were analyzed in triplicate during qPCR using the StepOnePlus Real-Time PCR System (Applied Biosystems). Each reaction contained 10 µL Fast SYBR® Green Master Mix (Applied Biosystems), 1 µL forward primer (20 pmol/µL), 1 µL reverse primer (20

pmol/μL), 7 μL nuclease-free water, and 1 μL cDNA template (2.5 ng/μL). The amplification program consisted of preincubation at 95°C for 20 s followed by 40 cycles of denaturation at 95°C for 3 s and annealing/extension at 64°C for 30 s. Melting curve analysis was performed to confirm single product amplification. The expression of three housekeeping genes (*RPS18* (Ribosomal Protein S18), *GAPDH* (Glyceraldehyde 3-phosphate dehydrogenase), *SUZ12* (SUZ12 polycomb repressive complex 2 subunit)) was tested in this study using NormFinder (Andersen et al., 2004) and PROC MIXED procedure of SAS (v9.2; SAS Institute Inc., Cary, NC). We chose *SUZ12* because it was the most stably expressed between and within the two groups. For each sample, the average Ct (Cycle threshold) of the *SUZ12* housekeeping gene was subtracted from the average Ct of the target gene to calculate ΔCt. A low ΔCt indicates high expression and vice versa. An unpaired t-test in SAS (SAS Institute Inc.) was used to analyze whether a gene showed significant difference between RFI groups.

3.1.8 DNA Extraction

Total DNA was extracted and used to quantify the relative mitochondrial genome copy numbers. The DNA was extracted from the rumen papillae (~80 mg) of 104 animals (35 L-RFI, 34 M-RFI, 35 H-RFI) using a bead beating, phenol-chloroform method as described by Li et al., 2012. Briefly, each sample was placed in a 2-mL microcentrifuge tube containing zirconium beads (0.3 g; 0.1 mm diameter) and washed twice with 1 mL of TN150 buffer (10 mM Tris-HCl [pH 8.0], 150 mM NaCl) by vortexing and centrifugation at 14,600 g for 5 min at 4°C. The tissue was then resuspended in 1 mL of TN150 and the Mini-BeadBeater-8 (BioSpec products, Bartlesville, OK) was used to mechanically disrupt cells at 5,000 rpm for 3 min. After bead beating, samples were immediately placed on ice and washed two times by phenol and chloroform-isoamyl alcohol (24:1). The DNA was then precipitated at -20°C overnight using

cold 100% ethanol and 3M sodium acetate. After precipitation, DNA was washed two times with 70% ethanol and dissolved in 30 μL nuclease-free water. The DNA concentration and quality was measured using Nanodrop (Thermo Scientific).

3.1.9 qPCR determination of relative mitochondrial DNA copy number per cell

The relationship between RFI and the relative copy number of mitochondrial DNA (mtDNA) per cell of the rumen epithelium was performed using correlation analysis. The ratio of mtDNA to nuclear DNA (nDNA) was used to determine the relative copy number of mtDNA per cell. We selected the *ND1* (NADH dehydrogenase subunit 1) gene as the mtDNA target (GenBank accession number: NC_006853, Location: 3101-4056) and the single copy, *DDX3Y* (DEAD box polypeptide 3, Y-linked) gene as the nDNA target (GenBank accession number: AC_000187, Location: 3458510 - 3468728,). The *ND1* primer sequences used to amplify a 200 bp product were 5-GAAC CACTACGACCCGCTACA-3 (forward), 5-GAGTTGGAAGCTCAGCCTGATC-3 (reverse) and the *DDX3Y* primer sequences used to amplify a 136 bp product were 5-ATCGTGGGCGGAATGAGTGT-3 (forward), 5-CTTGGTGGAAGCGGTTTTGA-3 (reverse) (Yue et al., 2014).

For qPCR, a standard curve was generated for both the mtDNA and nDNA. First, PCR was performed on pooled DNA to amplify mtDNA and nDNA separately. The PCR mix contained 50 ng/μL DNA along with 10X PCR buffer, 50 mM $MgCl_2$, 10 mM dNTP, 20 pmol of each primer, Taq polymerase, and nuclease-free water to a final volume of 50 μL. The PCR program consisted of 1 cycle 94˚C for 5 min, 30 cycles of 94˚C for 30 sec, 62˚C for 30 sec, 72˚C for 30 sec and 1 cycle of 72˚C for 7 min with hold at 4˚C. Each PCR product was then subjected to agarose gel electrophoresis in order to excise DNA bands for purification using the QIAquick Gel Extraction Kit (Qiagen). The concentration of the purified mtDNA and nDNA was measured

by Nanodrop (Thermo Scientific) and an eight-point standard curve with 10 fold dilutions was created for each. DNA copy number of the standard curve points was calculated as described by Speicher and Johnson (2012). Expression of mtDNA and nDNA within 104 samples (35 L-RFI, 34 M-RFI, 35 H-RFI) was then analyzed by qPCR along with their respective standard curve using an annealing temperature of 62˚C. DNA copy number within samples was extrapolated from the standard curve and all samples and standard curves were analyzed in triplicate. A one-way ANOVA was performed in SAS (SAS Institute Inc.) to compare RFI groups. Also, a Pearson correlation analysis of relative mitochondrial DNA copy number per cell and RFI was performed in SAS (SAS Institute Inc.) and R (R Core Team, 2014).

3.2 Results

3.2.1 Summary of the rumen epithelial transcriptome

On average there were 42 million high-quality, paired reads generated per sample (mean ± SD = 41,991,418 ± 6,835,817) from RNA-seq and the overall read alignment rate to the bovine reference genome was 85% ± 3.72%. The total number of genes expressed (genes with at least one read in at least one sample) within the rumen epithelium was 22,338 with an average of 14,677 ± 1,062 genes per L-RFI sample and 16,239 ± 1,326 per H-RFI sample. There were 11,284 core genes among samples and of these core genes, 9,700 were annotated by PANTHER. The top molecular functions for the core genes were catalytic activity and binding, which included 30.7% and 30.1% of the core genes, respectively. In the biological processes category, 32.6% of the core genes were involved in cellular process and 47.5% of the genes were associated with metabolic process.

3.2.2 Clustering of RFI groups

The PCA plot (Figure 3.1) shows that L-RFI and H-RFI gene expression profiles seem to fall into somewhat distinct clusters. However, there was a L-RFI outlier sample (271L) that did not cluster with the rest of the samples, which may possibly be related to the animal's low ADG and EndWT (Figures 3.1 and 3.2). Hierarchical clustering by WGCNA showed that all the L-RFI samples clustered together while the H-RFI samples did not (Figure 3.2). When comparing animals with similar ADG and EndWT in the trait heat map, L-RFI individuals had lower RFI, DMI and MEI than H-RFI individuals. The means of the two groups for all traits (Supplementary table 3.1) were compared and there was no significant difference in BirthWT, WeanWT, MWT, EndWT, CWT, and ADG. However, the L-RFI group had significantly ($p < 0.001$) lower RFI, DMI and MEI by 3.82 kg/day, 3.86 kg/day and 4.68 Mcal/day, respectively.

3.2.3 Differential gene expression in rumen epithelium between low- and high- RFI cattle

There were 122 genes DE in the rumen epithelial tissues between L- and H- RFI animals (Supplementary table 3.2). Of these DE genes, 85 were up-regulated and 37 down-regulated in the L-RFI group. DAVID annotation of the 122 DE genes found no significant KEGG pathways, however the biological term acetylation was significantly enriched (FDR<0.05). A total of 30 DE genes were involved in the process of acetylation, 26 of which were up-regulated and 4 down-regulated in L-RFI animals (Table 3.2). These genes have functions in protein synthesis (i.e. *RPL10*, *RPS15*, *RPL36*), protein degradation (i.e. *PSMB6*, *UBC*/*UBA52*, *UBE2V1*), cytoskeletal organization (i.e. *DSTN*, *ACTB*, *TUBB5*, *TMSB10*), energetic substrate generation (i.e. *TECR*, *TPI1*), and stress response (i.e. *HSPB1*, *HSF1*).

Ingenuity analysis of the 85 differentially up-regulated genes in L-RFI samples showed that the top significantly enriched canonical pathway was remodeling of the epithelial adherens

junctions through endocytosis (i.e. *DNM2*), degradation (i.e. *HGS*), and cytoskeletal organization (i.e. *ACTB*, *TUBB*, *TUBA4A*) (Table 3.3, Supplementary table 3.2). The other enriched canonical pathways were involved in functions such as protein synthesis (eIF2 signaling), cytoskeletal dynamics, cell growth, proliferation, apoptosis, and migration (signaling by Rho family GTPases, RhoGDI signaling, ephrin B signaling) (Table 3.3). For the 37 DE genes that were down-regulated in L-RFI animals, the top significant canonical pathways were metabolic processes such as 4-aminobutyrate degradation I (i.e. *SUCLG2*), glutamate degradation III (via 4-aminobutyrate; i.e. *SUCLG2*), inositol pyrophosphates biosynthesis (i.e. *PPIP5K2*), superpathway of inositol phosphate compounds (i.e. *PPIP5K2*, *NUDT12*), and NAD salvage pathway II (i.e. *NUDT12*) (Table 3.3).

3.2.4 qPCR validation of selected DE genes

To show the reliability of the differential gene expression analysis of DESeq2, we further selected five DE genes for validation using qPCR. Of these five genes, four (*TECR*, *COX8A*, *SLC25A39*, *PKM2*) had significantly greater expression (i.e. Lower ΔCt, $p<0.05$) in L-RFI while one (*TPI1*) tended to have significantly greater expression ($p<0.1$) (Table 3.4). These results were in agreement with the differential expression analysis of DESeq2 in that the genes had greater expression in L-RFI rumen epithelium.

3.2.5 Identification of WGCNA gene co-expression modules correlated with RFI

WGCNA was conducted to identify gene co-expression modules that are correlated with RFI. We identified a total of eight gene modules that were correlated with RFI, excluding a grey module that contained genes that did not belong to any other module (Figure 3.3). The Brown and Green modules had a significant positive correlation with RFI ($r = 0.54$, $p = 0.02$, 162 genes for Brown module and $r = 0.51$, $p = 0.03$, 133 genes for Green Module, respectively) while the

Turquoise module had a significant negative correlation with RFI ($r = -0.50$, $p = 0.03$, 764 genes). Functional analysis of the genes enriched in the Green module did not result in any significantly enriched biological functions or pathways while there was only one significant biological term, which was muscle protein containing four genes in the Brown module. Many significant functions were associated with the turquoise module (Tables 3.5 and 3.6) and therefore this study focused on functional examination of the 764 genes enriched in this module, which had greater expression in the L-RFI epithelium.

When functional analysis was performed using DAVID, 20 biological functions and 6 KEGG pathways were significantly enriched for genes in the turquoise module (Table 3.5). The most significant biological functions were acetylation (195 genes) and phosphoprotein (210 genes), which are involved in post-translational modification. Many of the other significant biological functions identified were also involved in protein related processes such as protein synthesis (i.e. ribosomal protein (44 genes), protein biosynthesis (20 genes)), degradation (i.e. proteasome (15 genes), threonine protease (7 genes)), folding (i.e. chaperone (17 genes)), and transport (i.e. transit peptide (35 genes), protein transport (24 genes)). In addition, biological terms associated with energy catabolism (i.e. ATP-binding (50 genes)) and anabolism (i.e. mitochondrion (47 genes)) were also identified. KEGG analysis of the 195 genes within the acetylation category indicated significant involvement of the acetylation related genes in ribosome and proteasome pathways. These pathways were also significantly enriched in the turquoise module along with oxidative phosphorylation, adherens junction, regulation of actin cytoskeleton, and spliceosome (Table 3.5). In the adherens junction pathway, there were 14 genes from the turquoise module that may regulate both the strong and weak adhesion between cells (Figure 3.4).

Further functional analysis using IPA showed that the top five most significant molecular and cellular functions for the genes in the turquoise module were protein synthesis, cellular growth and proliferation, post-translational modification, protein folding and cell death and survival (Table 3.6). Furthermore, the top canonical pathways were eIF2 signaling, regulation of eIF4 and p70S6K signaling, mTOR signaling and epithelial adherens junctions remodeling and signaling (Table 3.6). IPA also generated a top toxicity list for the genes in the turquoise module, which contained processes such as mitochondrial dysfunction and biogenesis, NRF2-mediated oxidative stress response, increased transmembrane potential of mitochondria and gene regulation by peroxisome proliferators via PPARα (Table 3.6).

Additionally, many genes from the turquoise module are involved in energy generating pathways such as glycolysis, tricarboxylic acid (TCA) cycle, and oxidative phosphorylation (Table 3.7). We also found three DE genes involved in glycolysis and three associated with oxidative phosphorylation, which were up-regulated in the L-RFI epithelium (Table 3.7). The DE genes involved in glycolysis are *TPI1* (Fold Change (FC; L-RFI/H-RFI)=1.24), *HK1* (FC=1.23), and *PKM2* (FC=1.30) while the DE genes involved in oxidative phosphorylation are *COX8A* (FC=1.28), *ATP6AP1* (FC=1.39), and *ATP6V0D1* (FC=1.26) (Table 3.7, Supplementary table 3.2).

3.2.6 Relative mtDNA copy number and RFI

The transcriptome analysis results showed up-regulation of genes in the L-RFI epithelium involved in mitochondrial functions such as oxidative phosphorylation, and mitochondrial dysfunction and biogenesis. Therefore, we speculated that L-RFI animals would have more relative mtDNA copy numbers (mtDNA/nDNA) in the rumen epithelium than H-RFI animals. To determine the relationship between RFI and relative mtDNA copy number, we included M-

RFI (n=34) animals along with L-RFI (n=35) and H-RFI (n=35) animals. The correlation analysis showed a significant positive relationship ($r = 0.21$, $p = 0.03$) between RFI and the relative mtDNA copy number per cell in the rumen epithelium (Figure 3.5). The epithelium of L-RFI animals had 741 ± 35 (mean ± SD) relative mtDNA copy numbers per cell while the epithelium of M- and H- RFI animals had 1,104 ± 89 and 1,000 ± 80, respectively. There was a significantly greater copy number of mtDNA in the rumen epithelium of M- and H- RFI animals compared to L-RFI animals ($p < 0.01$). However, no significant difference in mtDNA copy number was observed between M- and H- RFI animals ($p > 0.05$).

3.3 Discussion

Improving cattle feed efficiency through selection for L-RFI could greatly reduce feed expense and increase profit for producers. Our study of steers divergent in RFI showed that L-RFI individuals are more feed efficient compared to H-RFI individuals because they were able to consume 3.82 kg less dry matter per day for similar growth, body weight, and carcass weight. These results coincide with those of others, which found that selection of L-RFI steers with 3.77 kg per day lower feed intake than H-RFI steers may lead to savings of $45.60 per head over a 120-day finishing period and there was no correlation of RFI with growth, body weight and carcass weight (Basarab et al., 2003). The difference in feed consumption between L- and H-RFI steers for similar production illustrates that differences may exist in the efficiency of feed conversion into energy and in the distribution of energy for growth, maintenance, and activity requirements. Studies have shown that the rumen microbial community differs between L- and H- RFI steers and may impact feed digestion and fermentation (Guan et al., 2008), which conservatively accounts for 10% of the variation in RFI (Richardson and Herd, 2004). Although

differences in the rumen microbial community have been associated with divergence in RFI, it is unknown whether there are differences in the rumen tissue that contribute to variation in RFI.

Our study found that 47.5% of the core genes among the rumen epithelial tissues of beef steers are involved in metabolic processes. These results indicate that rumen epithelial cells may have many metabolic functions. Indeed, the rumen epithelium was known to be highly metabolic because it contains a high density of mitochondria in the stratum basale layer (Graham and Simmons, 2005) and metabolizes a large proportion of absorbed SCFAs (Sehested et al., 1999). We predicted there might be differences in the expression of genes involved in metabolic processes that generate energy as well as differences in nutrient absorption between steers divergent in RFI. Through hierarchical clustering, we found that the whole transcriptome profiles of the rumen epithelial tissues of H-RFI (inefficient) steers did not cluster together while all L-RFI (efficient) steers did. This indicates that the rumen epithelial transcriptome of H-RFI animals are more variable and there are similarities among the gene expression profiles of L-RFI animals that may be associated with higher feed efficiency.

We had hypothesized that there was greater expression of genes involved in absorption of SCFAs from the rumen of L-RFI animals. However, we did not find evidence of differences in the expression of known or candidate SCFA transporters belonging to solute carrier (*SLC*) gene families such as *SLC4A*, *SLC16A* (monocarboxylate transporters), *SLC21A*, *SLC22A*, or *SLC26A* (Aschenbach et al., 2009) between the L- and H- RFI animals in this study (data not shown). Although we did not observe differences in protein-mediated SCFA transport, our results do show evidence of differences that may affect paracellular permeability and impact simple diffusion of SCFAs and other nutrients. For example, we found up-regulated pathways in the L-RFI epithelium such as regulation of actin cytoskeleton and epithelial adherens junctions remodeling and signaling that are important in modulating cell-cell adhesion and may therefore

affect paracellular permeability (Takeichi, 1990; Guo et al., 2003). The components of adherens junctions that were encoded by genes with greater expression in the L-RFI epithelium consisted of the plasma membrane cell adhesion molecules (*CAMs*), E-cadherin and nectin, as well as intracellular regulators of these molecules such as *p120ctn*, *v-Src*, *IQGAP1*, and *ACTB*. CAMs require attachment to the actin cytoskeleton in order to mediate cell adhesion (Vasioukhin et al., 2000). For example, E-cadherin are anchored to actin via the intracellular proteins, α- and β-catenin, while nectin is anchored via afadin (Nathke et al., 1994; Kurita et al., 2011). Additionally, E-cadherin requires interaction with a key regulator, p120ctn, in order to promote strong adhesion between cells (Thoreson et al., 2000). In our study, the L-RFI epithelium had increased expression of the *p120ctn* regulator, however, there was also increased expression of negative regulators such as *v-Src* and *IQGAP1* that promote weak adhesion. IQGAP1 weakens adhesion by stimulating dissociation of the cadherin-catenin complex (Kuroda et al., 1998) and v-Src dissociates both the cadherin-catenin and cadherin-p120ctn complexes by phosphorylation (Ozawa and Ohkubo, 2001; Piedra et al., 2001).

Furthermore, we found several DE genes that were up-regulated in the L-RFI epithelium encoding Dynamin-2 (*DNM2*), Hepatocyte growth factor-regulated tyrosine kinase substrate (*HGS*), and cytoskeletal components (Beta-actin (*ACTB*), Tubulin beta-5 (*TUBB5*), and Tubulin alpha-4a (*TUBA4A*)) that are also involved in remodeling of epithelial adherens junctions. Dynamin-mediated internalization of E-cadherin through endocytosis is known to play an important role in weakening adhesion between cells (Paterson et al., 2003; Troyanovsky et al., 2006) and cytoskeletal components are essential for endocytosis to occur (Apodaca, 2001). Activation of HGS via v-Src subsequently targets internalized E-cadherin to lysosomes for degradation (Palacios et al., 2005). The regulation of intercellular adhesion strength and the actin cytoskeleton are vital to many processes such as cell migration, tissue remodeling, and

maintenance of tissue integrity (Baum and Georgiou, 2011). We found up-regulated DE genes (*RHOG*, *CFL1, ACTB*, *MYL12B*, *GNB1*, *GNB2*, *MAPK1*) in the L-RFI epithelium involved in several important signaling pathways regulating cell migration including signaling by Rho family GTPases, RhoGDI, and Ephrin B that mediate their effect on cell migration though modulation of intercellular adhesion and regulation of the actin cytoskeleton (Ridley, 2001; Dovas and Couchman, 2005; Park and Lee, 2015). Overall, the increased expression of genes related to modulation of intercellular adhesion strength, cytoskeletal organization, and cell migration signaling pathways suggest there is greater cell mobility and dynamic remodeling within the L-RFI epithelium, which may create gaps between cells resulting in a leakier epithelium and greater paracellular permeability for the absorption of nutrients. Increased nutrient absorption would provide more substrates for whole body energy production and may be a contributing factor to the high feed efficiency of L-RFI animals.

Tissue morphogenesis is a process that involves changes to the number, shape, size, position, and gene expression of cells in order to develop and maintain a tissue (Heisenberg and Bellaïche, 2013). Increased modulation of intercellular adhesion, cell migration, and cytoskeletal organization indicate greater tissue morphogenesis in the L-RFI epithelium. Additional evidence from our transcriptome analyses results also support that the rumen epithelium of L-RFI animals have greater tissue morphogenesis compared to H-RFI animals. For instance, we found up-regulation of functions such as cellular growth, proliferation, and death in the L-RFI epithelium, indicating increased cell turnover. There was also up-regulation of protein synthesis, degradation, folding, transport, and post-translational modification processes that suggest increased protein turnover. Greater tissue morphogenesis and paracellular permeability in the L-RFI epithelium may possibly be due to a greater ruminal supply of SCFAs. It has been found that L-RFI animals have a greater concentration of total SCFAs ($p=0.059$) in the rumen fluid with

significantly greater concentrations of butyrate ($p<0.001$) and valerate ($p=0.006$) (Guan et al., 2008). The increased nutrient availability in L-RFI animals may be attributed to greater feed digestibility and fermentation by rumen microbes (Nkrumah et al., 2006; Guan et al., 2008). High SCFA concentrations lead to enhanced absorption by simple diffusion due to decreased pH and an increased concentration gradient between the lumen and blood (López et al., 2003). Steele and colleagues (2011) have observed changes in the epithelium such as large intercellular spaces, extensive sloughing of surface epithelial cells, and increased cell migration associated with high SCFA concentrations in the rumen. Additionally, it has been found that high SCFA concentrations increased rumen epithelial cell proliferation (Goodlad, 1981). These studies showed that high SCFA concentrations and the associated decrease in pH resulted in an increased rate of surface epithelial cell sloughing, however there was increased cell proliferation and migration possibly to replace sloughed cells and maintain tissue barrier integrity (Goodlad, 1981; Steele et al., 2011). It was suggested that the large gaps between epithelial cells would increase the paracellular transport of SCFAs from the rumen (Steele et al., 2011). Therefore, the increased tissue morphogenesis we observed in the L-RFI epithelium may be a response to high SCFA concentrations and/or metabolic stress caused by increased nutrient availability. Greater tissue morphogenesis may result in increased paracellular permeability of the epithelium for the absorption of SCFAs and other nutrients.

Although our study suggests that the L-RFI epithelium may have increased paracellular permeability for SCFA absorption, we did not find any difference between RFI groups in the expression of genes in the epithelium involved in ketogenesis or beta-oxidation of SCFAs. This indicates that there may be a greater concentration of SCFAs entering the portal blood of L-RFI animals to be metabolized by other tissues, however there have been no studies yet measuring differences in the appearance of SCFAs in the portal blood between RFI groups. While we did

not observe a difference in beta-oxidation, we found up-regulation of genes in the L-RFI epithelium involved in energy generating pathways such as glycolysis, TCA cycle, and oxidative phosphorylation. Similarly, butyrate supplementation increased expression of genes involved in glycolysis and oxidative phosphorylation in the rumen (Laarman et al., 2013). It was suggested that butyrate induced energy mobilization to maintain tissue barrier integrity in the presence of high SCFA concentrations (Laarman et al., 2013), which may be happening in the L-RFI epithelium because they are exposed to a significantly greater concentration of butyrate (Guan et al., 2008).

The majority of cellular energy, in the form of ATP, is generated through oxidative phosphorylation within the mitochondrial inner membrane (Alberts et al., 2002). Because our results show that the L-RFI epithelium has increased expression of genes encoding mitochondrial proteins involved in oxidative phosphorylation, it suggests L-RFI beef steers have increased energy production in the rumen epithelium. This may also indicate higher mitochondrial activity and/or greater mitochondrial genome copy numbers in the rumen epithelium of L-RFI steers compared to H-RFI steers. However, we found RFI was positively correlated ($r = 0.21$, $p = 0.03$) to the mitochondrial genome copy number per cell of the epithelium. The increased expression of oxidative phosphorylation genes, but lower mitochondrial genome copy numbers may indicate increased mitochondrial efficiency for the generation of energy in L-RFI animals. Although we could not directly measure mitochondrial activity in our study, others have reported a more rapid rate of oxidative phosphorylation in the mitochondria of skeletal muscle and the liver in L-RFI beef cattle (Kolath et al., 2006; Lancaster et al., 2014). We speculate that the mitochondria in the L-RFI rumen may also have the same capability, which needs to be further studied. We found up-regulation of functions such as mitochondrial dysfunction, biogenesis of mitochondria, and NRF2-mediated oxidative stress response that may indicate increased mitochondrial activity and

metabolic stress in the L-RFI epithelium. For example, increased mitochondrial activity leads to greater production of reactive oxygen species, resulting in oxidative stress and initiation of oxidative stress responses (Murphy, 2009). High oxidative stress may cause mitochondrial dysfunction and activation of apoptotic signaling molecules to remove damaged mitochondria. The damaged mitochondria are replaced by healthy mitochondria in order to maintain metabolic function. Overall, increased expression of glycolytic and oxidative phosphorylation genes in the L-RFI epithelium suggests increased energy production. The increased energy production provides a resource for the increased tissue morphogenesis occurring to maintain barrier integrity in the L-RFI epithelium, which is an energetically expensive process.

Additionally, our study showed significant enrichment of genes in the L-RFI epithelium associated with the post-translational modification process, acetylation. These genes were involved with various processes such as protein synthesis, protein degradation, cytoskeletal organization, metabolism of energetic substrates, and stress response. This suggests that acetylation modulates genes belonging to a wide range of processes and these processes are cellular responses to high levels of nutrients. Acetylation is known to be a metabolically sensitive protein modification process important in the cellular response or adaptation to metabolic stress caused by nutrient excess (Wellen and Thompson, 2010). Because there was an increased expression of genes in the L-RFI epithelium that could be acetylated with functions in cellular response to metabolic stress, it suggests that the L-RFI individuals have a greater nutrient supply to the rumen epithelium for higher energy production.

In conclusion, the rumen epithelium may contribute to variation in RFI through differences in the expression of genes that affect the paracellular transport of nutrients. The increased expression of genes in the L-RFI epithelium involved in modulation of adherens junctions, cytoskeletal organization, and cell migration signaling pathways may cause large

intercellular gaps and result in greater paracellular absorption of nutrients. The L-RFI epithelium showed increased tissue morphogenesis as characterized by increased expression of genes involved in cell and protein turnover, modulation of intercellular adhesion strength, and cell migration, which may be a response to metabolic stress or the acidic effects of high SCFA concentrations in the L-RFI rumen. There was no difference in SCFA metabolism; however, there was increased expression of genes associated with glycolysis and oxidative phosphorylation in the L-RFI epithelium suggesting greater energy production. The increase in energy production provides a resource for the dynamic processes involved in maintaining tissue barrier integrity.

Table 3.1. Gene name, accession number, functional pathway, primer sequences, and product length of selected genes used in qPCR validation.

Gene name (symbol)	GenBank accession number	Functional pathway	Forward and reverse primer sequence (5'-3')	Product length (bp)	Reference
Triosephosphate Isomerase 1 (*TPI1*)	NM_001013589	Glycolysis, Gluconeogenesis, Acetylation	Fwd: GGGAGGAAGAACAATCTGGGG Rev: GCGAAGTCAATGTAGGCGGT	107	This study
Trans-2,3-Enoyl-CoA Reductase (*TECR*)	NM_001034748	Biosynthesis of unsaturated fatty acids, Acetylation	Fwd: CCAAGGGCAAGTCCCTGAAG Rev: AGGTCCCGGAAGTAGAGTGT	82	This study
Cytochrome C Oxidase Subunit VIIIA (*COX8A*)	NM_174024	Oxidative Phosphorylation	Fwd: TTTGACTTCGCGACCTTGG Rev: TTACGGCACGGAGTAGACTG	60	This study
Solute Carrier Family 25 Member 39 (*SLC25A39*)	NM_001075415	Mitochondrial substrate/solute carrier	Fwd: AGCTAATGCCTCCCTCCAGA Rev: GGCACTTCCATTTGGCGTAG	54	This study
Pyruvate Kinase M2 (*PKM2*)	NM_001205727	Glycolysis, Gluconeogenesis	Fwd: TGTCACCCATTACCAGCGAC Rev: TATCTGGCCACCTGATGTGC	130	This study
SUZ12 polycomb repressive complex 2 subunit (*SUZ12*)	NM_001205587	Endogenous control	Fwd: CATCCAAAAGGTGCTAGGATAGATG Rev: TGGGCCTGCACACAAGAATG	160	Rekawiecki et al., 2012

Table 3.2. Rumen epithelial DE genes between L-RFI and H-RFI that are significantly (FDR<0.05) involved in acetylation as identified by DAVID.

Ensembl ID	Gene symbol	Gene name	Fold change*	FDR adjusted p-value
ENSBTAG00000005654	*TMSB10*	Thymosin beta 10	1.44	1.28E-02
ENSBTAG00000012632	*TECR*	Trans-2,3-enoyl-CoA reductase	1.43	1.02E-05
ENSBTAG00000030974	*TUBA4A*	Tubulin, alpha 4a	1.43	5.63E-04
ENSBTAG00000007454	*RPL10*	Ribosomal protein L10	1.40	2.03E-04
ENSBTAG00000011969	*HSPB1*	Heat shock 27kDa protein 1	1.34	1.28E-02
ENSBTAG00000013390	*PSMB6*	Proteasome (prosome, macropain) subunit, beta type, 6	1.32	1.41E-02
ENSBTAG00000016874	*DNAJB1*	DnaJ (Hsp40) homolog, subfamily B, member 1	1.29	1.28E-02
ENSBTAG00000019718	*RPS15*	Ribosomal protein S15	1.29	1.85E-03
ENSBTAG00000006969	*TUBB5*	Tubulin, beta	1.28	4.02E-02
ENSBTAG00000001794	*RPL36*	Ribosomal protein L36	1.28	2.49E-02
ENSBTAG00000020560	*CLPTM1*	Cleft lip and palate associated transmembrane protein 1	1.27	1.41E-02
ENSBTAG00000004379	*ETHE1*	Ethylmalonic encephalopathy 1	1.26	3.75E-02
ENSBTAG00000000411	*HGS*	Hepatocyte growth factor-regulated tyrosine kinase substrate	1.26	1.28E-02
ENSBTAG00000020751	*HSF1*	Heat shock transcription factor 1	1.26	2.84E-02
ENSBTAG00000021455	*CFL1*	Cofilin 1 (non-muscle)	1.26	1.41E-02
ENSBTAG00000014872	*CAPNS1*	Calpain, small subunit 1	1.26	1.36E-02
ENSBTAG00000016952	*PSMD5*	Proteasome (prosome, macropain) 26S subunit, non-ATPase, 5	1.26	4.07E-02
ENSBTAG00000026199	*ACTB*	Actin, beta	1.24	3.13E-02
ENSBTAG00000017246; ENSBTAG00000007737	*UBC; UBA52*	Ubiquitin C; Ubiquitin A-52 residue ribosomal protein fusion product 1	1.24	1.91E-02
ENSBTAG00000016024	*MYL9*	Myosin regulatory light polypeptide 9	1.24	6.77E-03
ENSBTAG00000019782	*TPI1*	Triosephosphate isomerase 1	1.24	3.56E-02
ENSBTAG00000006495	*GNB2*	Guanine nucleotide binding protein (G protein), beta polypeptide 2	1.24	4.89E-02
ENSBTAG00000027316	*UBE2V1*	Ubiquitin-conjugating enzyme E2 variant 1	1.23	4.02E-02
ENSBTAG00000015434	*DSTN*	Destrin (actin depolymerizing factor)	1.22	4.86E-02
ENSBTAG00000000215	*GNB1*	Guanine nucleotide binding protein (G protein), beta polypeptide 1	1.18	4.06E-02
ENSBTAG00000013362	*DNM2*	Dynamin 2	1.17	4.86E-02
ENSBTAG00000009780	*GTF2I*	General transcription factor II, i	0.85	4.86E-02
ENSBTAG00000009541	*SUCLG2*	Succinate-CoA ligase, GDP-forming, beta subunit	0.84	4.86E-02
ENSBTAG00000038488	*TMSB4*	Thymosin beta 4, X-linked	0.77	1.60E-03
ENSBTAG00000013982	*UACA*	Uveal autoantigen with coiled-coil domains and ankyrin repeats	0.72	2.11E-02

*Fold change is gene expression in L-RFI relative to H-RFI

Table 3.3. Top Ingenuity canonical pathways significantly enriched ($p<0.05$) for up-regulated and down-regulated DE genes in L-RFI rumen epithelium.

Ingenuity canonical pathways	p-value	Genes
Up-regulated		
Remodeling of Epithelial Adherens Junctions	6.11E-06	*ACTB, TUBB5, DNM2, TUBA4A, HGS*
Signaling by Rho Family GTPases	3.09E-05	*RHOG, CFL1, ACTB, MYL12B, GNB1, MAPK1, GNB2*
RhoGDI Signaling	5.19E-05	*RHOG, CFL1, ACTB, MYL12B, GNB1, GNB2*
eIF2 Signaling	7.53E-05	*UBA52, RPL36, MAPK1, RPL18A, RPS15, RPL10*
Ephrin B Signaling	1.74E-04	*CFL1, GNB1, MAPK1, GNB2*
Down-regulated		
4-aminobutyrate Degradation I	4.09E-03	*SUCLG2*
Glutamate Degradation III (via 4-aminobutyrate)	6.81E-03	*SUCLG2*
Inositol Pyrophosphates Biosynthesis	9.52E-03	*PPIP5K2*
Superpathway of Inositol Phosphate Compounds	2.89E-02	*PPIP5K2, NUDT12*
NAD Salvage Pathway II	3.49E-02	*NUDT12*

Table 3.4. Comparison of gene expression between the rumen epithelium of L- and H- RFI animals by qPCR.

Gene	L-RFI ΔCt (n=30)	H-RFI ΔCt (n=27)	p-value
TPI1	-3.23 ± 0.57	-2.99 ± 0.38	0.07
TECR	-2.36 ± 0.57	-2.00 ± 0.51	0.01*
COX8A	-7.85 ± 1.30	-6.57 ± 1.89	0.004*
SLC25A39	-3.67 ± 0.51	-0.24 ± 0.60	3.8E-30*
PKM2	-6.64 ± 0.58	-3.78 ± 0.53	4.4E-26*

Data are Mean ± SD

*p-value <0.05

Table 3.5. Biological functions and pathways significantly (FDR<0.05) enriched in the Turquoise module using DAVID.

DAVID functional category	Biological term	Number of genes	FDR adjusted p-value
SP_PIR_KEYWORD	Acetylation	195	8.22E-44
	Phosphoprotein	210	9.16E-19
	Ribonucleoprotein	51	3.63E-17
	Cytoplasm	138	1.17E-16
	Ribosomal protein	44	2.53E-16
	Protein biosynthesis	20	2.24E-06
	Isopeptide bond	23	5.54E-06
	Proteasome	15	8.76E-06
	Ubl conjugation	29	5.80E-05
	Nucleotide-binding	74	3.65E-04
	Wd repeat	22	8.04E-04
	Actin-binding	17	9.48E-04
	Transit peptide	35	4.94E-03
	Chaperone	17	6.61E-03
	Threonine protease	7	8.72E-03
	Methylation	17	1.67E-02
	Initiation factor	9	1.80E-02
	ATP-binding	50	2.43E-02
	Mitochondrion	47	3.18E-02
	Protein transport	24	3.47E-02
KEGG_PATHWAY	bta03010:Ribosome	36	3.05E-21
	bta03050:Proteasome	14	1.86E-05
	bta04520:Adherens junction	14	1.97E-03
	bta00190:Oxidative phosphorylation	19	5.94E-03
	bta04810:Regulation of actin cytoskeleton	22	2.65E-02
	bta03040:Spliceosome	16	3.95E-02

Table 3.6. Top biological functions and pathways significantly ($p<0.05$) enriched in the Turquoise module with IPA.

IPA category	Biological term	Number of genes	p-value
Molecular and cellular function	Protein synthesis	89	1.08E-14
	Cellular growth and proliferation	232	1.73E-14
	Post-translational modification	51	2.02E-10
	Protein folding	17	9.02E-10
	Cell death and survival	211	1.47E-09
Canonical pathway	EIF2 signaling	51	1.47E-32
	Regulation of eIF4 and p70S6K signaling	35	1.64E-20
	mTOR signaling	39	2.70E-20
	Remodeling of epithelial adherens junctions	19	4.83E-13
	Epithelial adherens junction signaling	25	1.59E-11
Toxicity list	Mitochondrial dysfunction	24	4.34E-09
	Biogenesis of mitochondria	5	4.14E-04
	NRF2-mediated oxidative stress response	17	2.26E-03
	Increases transmembrane potential of mitochondria and mitochondrial membrane	6	6.12E-03
	Mechanism of gene regulation by peroxisome proliferators via PPARα	7	3.94E-02

Table 3.7. Genes involved in major energy generating pathways that have increased expression in the rumen epithelium of L-RFI cattle.

Energy generating pathway	Gene symbol	Gene name	DE gene (D) and/or within turquoise module (T)
Glycolysis	*GPI*	Glucose-6-phosphate isomerase	T
	PFKL	Phosphofructokinase, liver	T
	ALDOA	Aldolase A, fructose-bisphosphate	T
	GAPDH	Glyceraldehyde-3-phosphate dehydrogenase	T
	TPI1	Triosephosphate isomerase 1	D, T
	HK1	Hexokinase 1	D
	PKM2	Pyruvate kinase M2	D
Tricarboxylic acid cycle	*CS*	Citrate synthase	T
	SUCLG1	Succinate-CoA ligase, alpha subunit	T
	ACO2	Aconitase 2, mitochondrial	T
	SDHB	Succinate dehydrogenase complex, subunit B	T
	DLAT	Dihydrolipoamide S-acetyltransferase	T
	ACLY	ATP citrate lyase	T
Oxidative phosphorylation	*ATP5D*	ATP synthase, H+ transporting, mitochondrial F1 complex, delta subunit	T
	COX7A2L	Cytochrome c oxidase subunit VIIa polypeptide 2 like	T
	ATP5J2	ATP synthase, H+ transporting, mitochondrial Fo complex, subunit F2	T
	NDUFA10	NADH dehydrogenase (ubiquinone) 1 alpha subcomplex, 10, 42kDa	T
	COX8A	Cytochrome c oxidase subunit VIIIA (ubiquitous)	D, T
	ATP6V1F	ATPase, H+ transporting, lysosomal 14kDa, V1 subunit F	T
	PPA1	Pyrophosphatase (inorganic) 1	T
	UQCRQ	Cytochrome b-c1 complex subunit 8	T
	NDUFB10	NADH dehydrogenase (ubiquinone) 1 beta subcomplex, 10, 22kDa	T
	NDUFS8	NADH dehydrogenase (ubiquinone) Fe-S protein 8, 23kDa (NADH-coenzyme Q reductase)	T
	ATP6AP1	ATPase, H+ transporting, lysosomal accessory protein 1	D, T
	ATP6V0D1	ATPase, H+ transporting, lysosomal 38kDa, V0 subunit D1	D, T
	ATP6V0E1	ATPase, H+ transporting, lysosomal 9kDa, V0 subunit E1	T
	COX10	Cytochrome c oxidase assembly protein	T
	COX4I1	Cytochrome c oxidase subunit IV isoform 1	T
	UQCRC1	Ubiquinol-cytochrome c reductase core protein I	T
	ATP6V0A1	ATPase, H+ transporting, lysosomal V0	T

	subunit A1	
NDUFV1	NADH dehydrogenase (ubiquinone) flavoprotein 1, 51kDa	T
PPA1	Pyrophosphatase (inorganic) 1	T
SDHB	Succinate dehydrogenase complex, subunit B, iron sulfur (Ip)	T

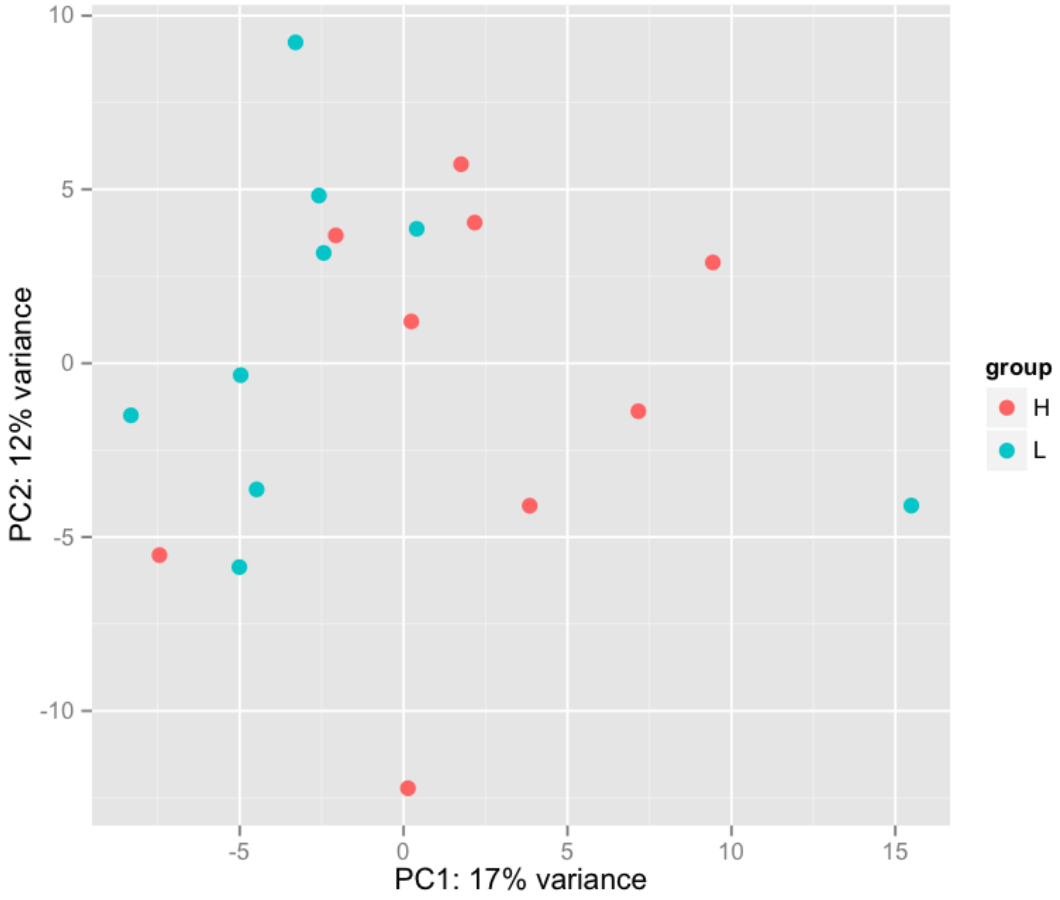

Figure 3.1. PCA plot of rumen epithelial transcriptomes from cattle with L-RFI (Blue, n=9) and H-RFI (Red, n=9). The samples are plotted along the first two principal components axis (PC1 and PC2).

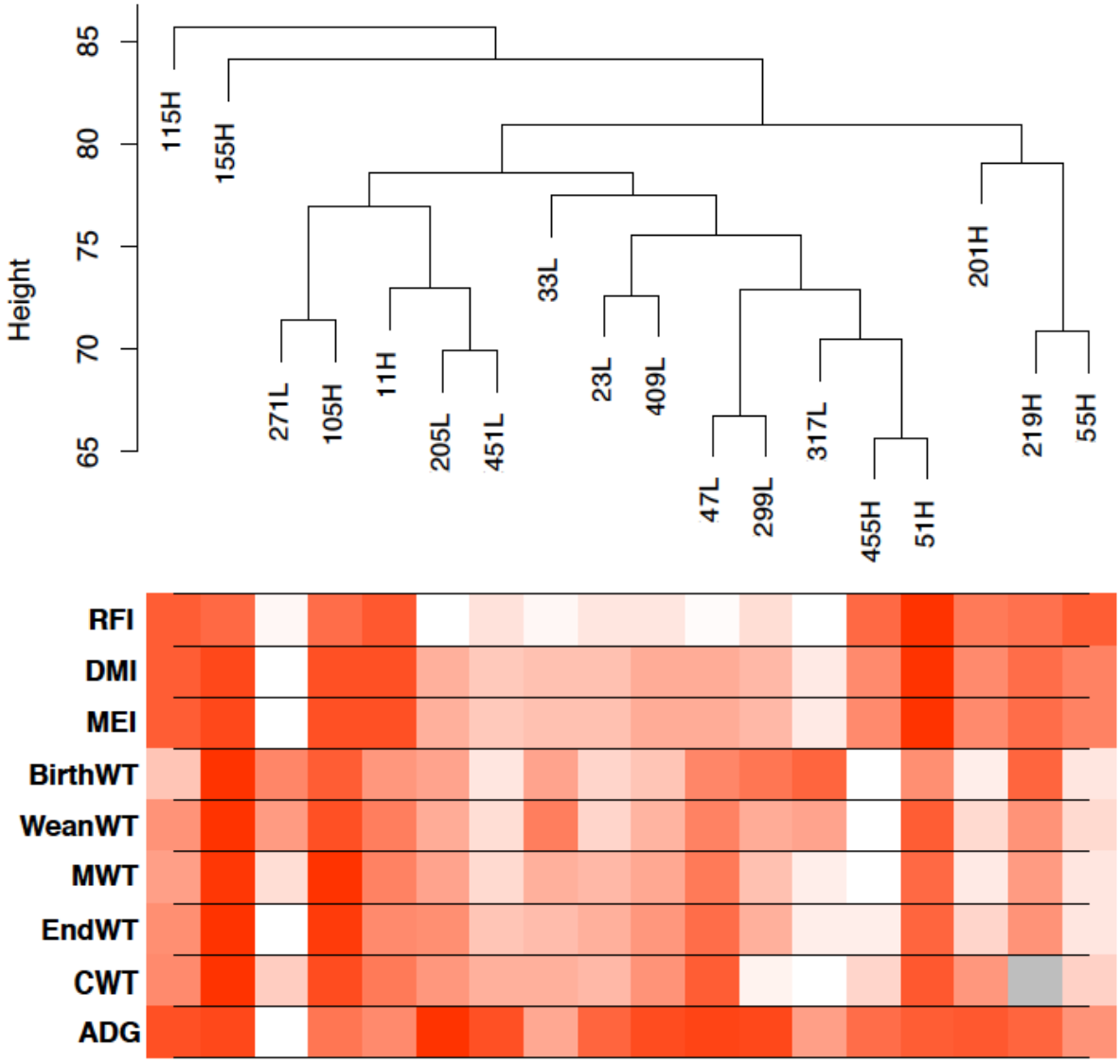

Figure 3.2. Hierarchical clustering dendrogram of rumen epithelial transcriptomes (9 L-RFI, 9 H-RFI) based on Euclidean distance and a trait heat map with a color gradient indicating trait levels. The gradient from white to dark red represents low to high levels of the trait while grey represents unavailable data. Traits examined were residual feed intake (RFI), dry matter intake (DMI), metabolizable energy intake (MEI), birth weight (BirthWT), weaning weight (WeanWT), metabolic mid-weight (MWT), end weight (EndWT), carcass weight (CWT), and average daily gain (ADG).

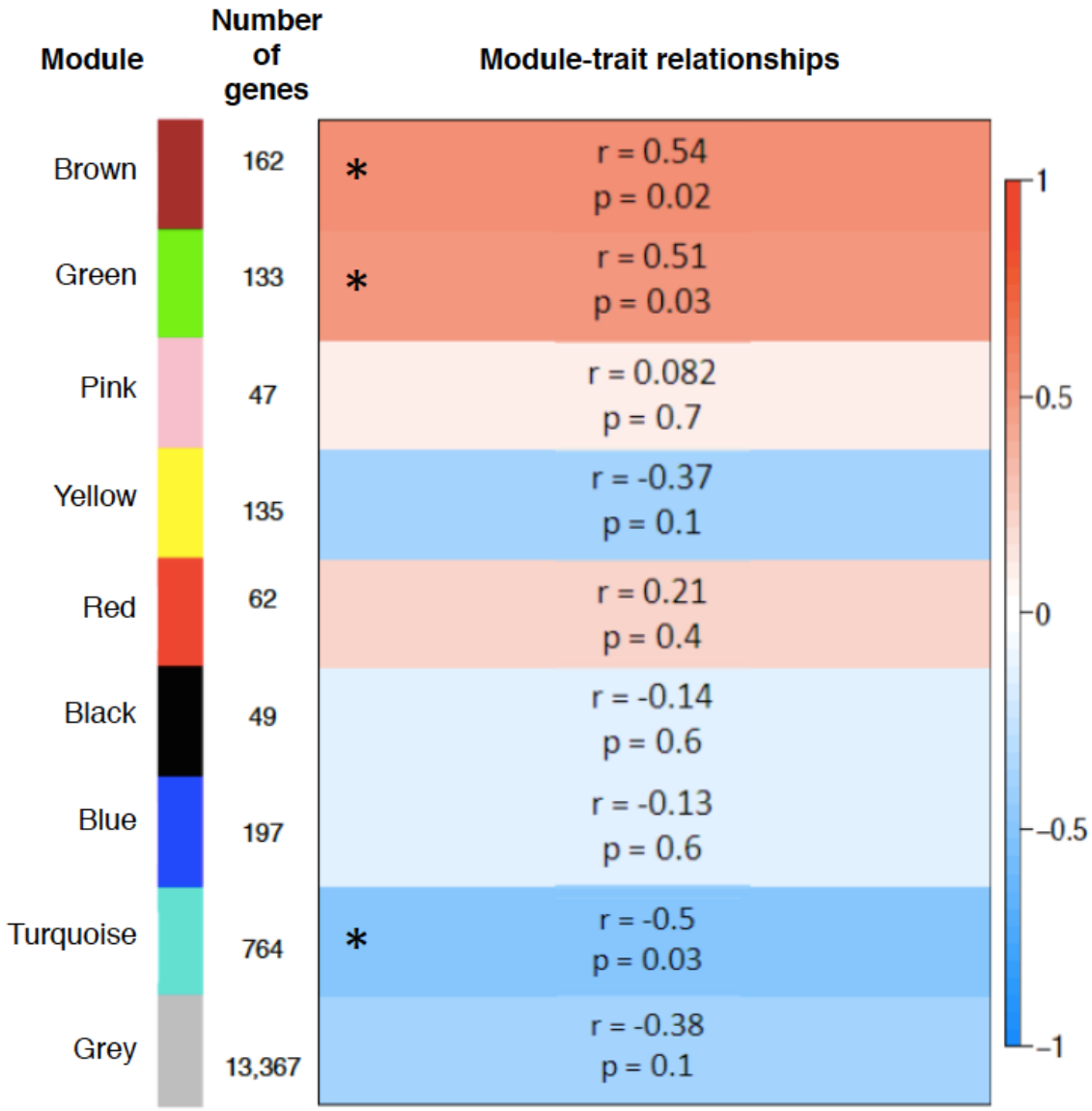

Figure 3.3. WGCNA identification of gene modules correlated with the RFI trait in the rumen epithelium of 18 steers (9 L-RFI, 9 H-RFI). Module names and sizes are shown along with the module-trait relationships indicating the correlation coefficients and p-values. The strength of the correlation is colored by different intensities of red (positive correlation) and blue (negative correlation). Asterisks indicate modules that are significantly ($p<0.05$) correlated with RFI.

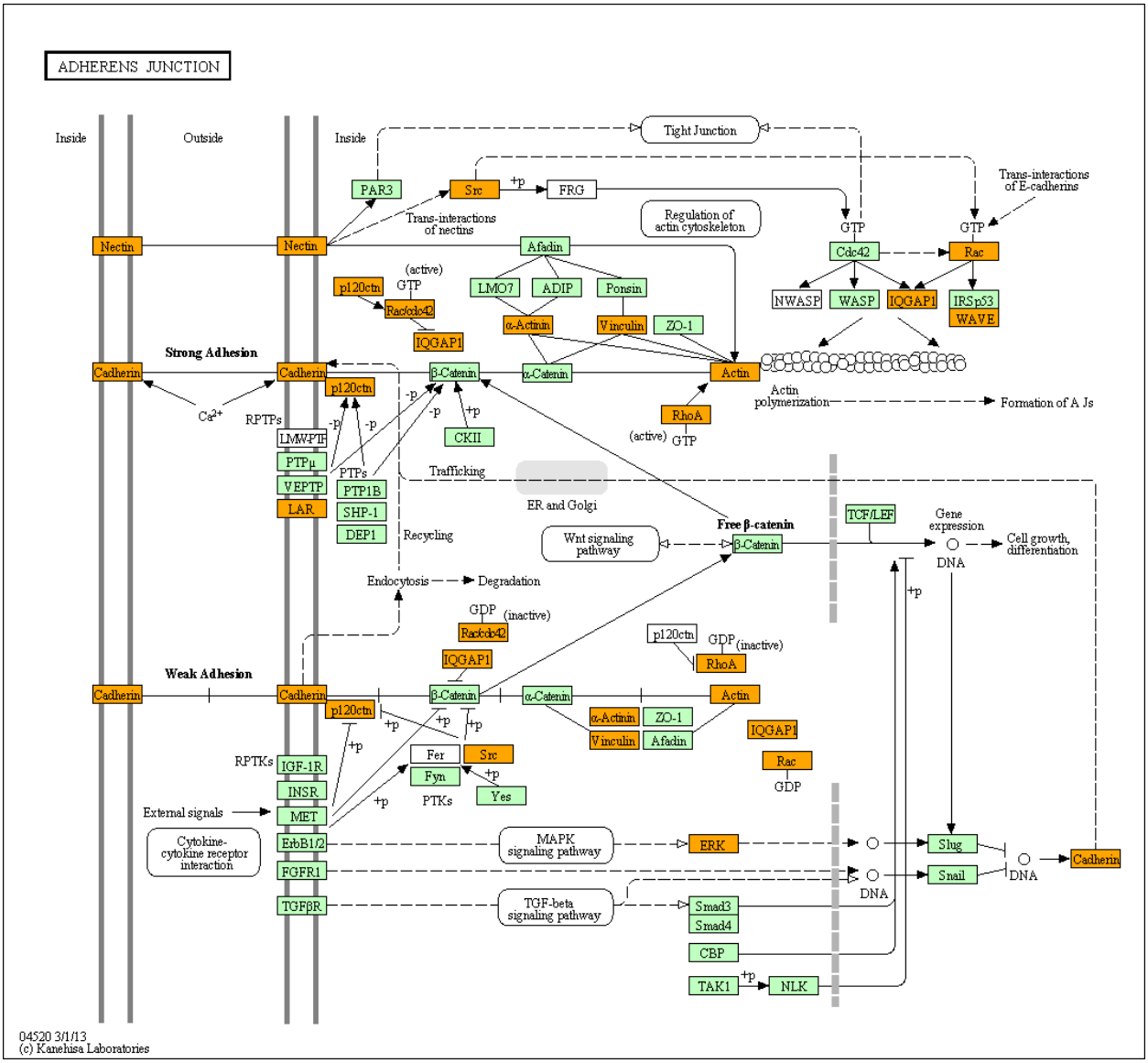

Figure 3.4. KEGG pathway for adherens junction. Genes within the turquoise module are shown in orange (Kanehisa and Goto, 2000; Kanehisa et al., 2014).

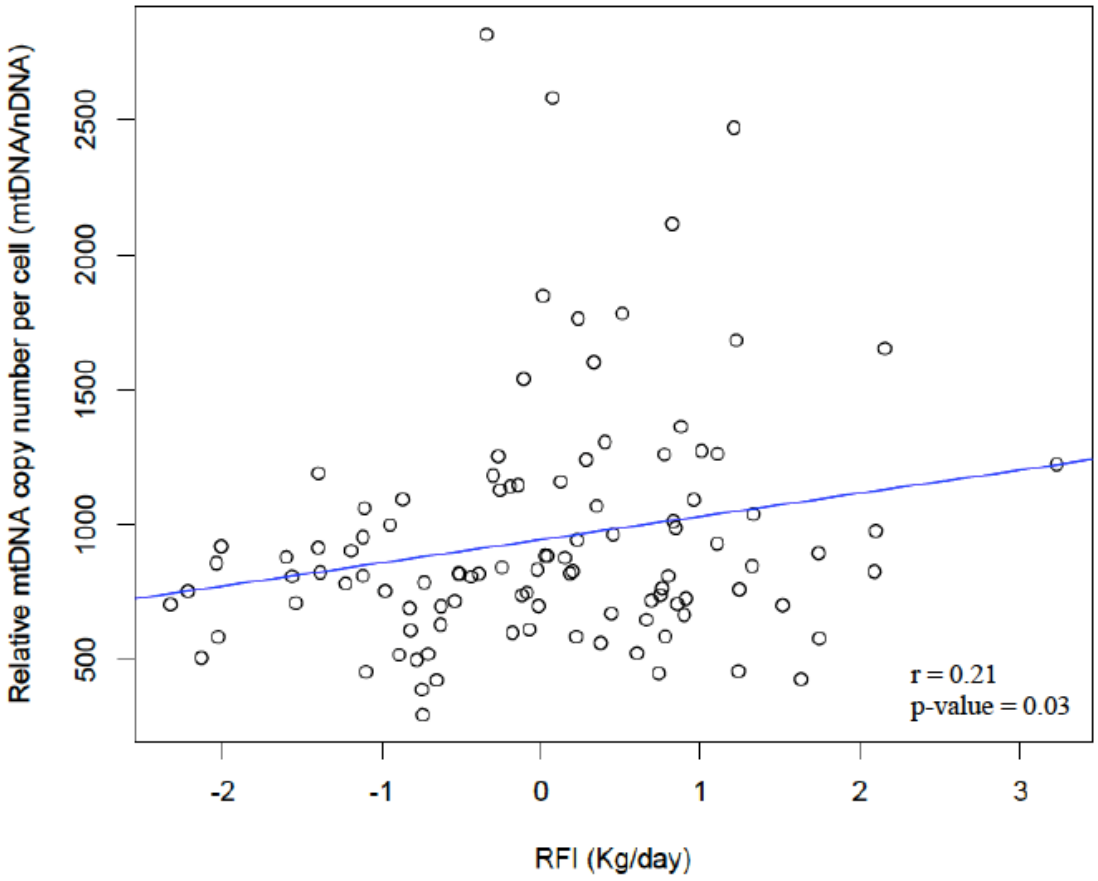

Figure 3.5. Correlation scatterplot of the relationship between relative mtDNA copy number per cell in the rumen epithelium (mtDNA/nDNA) and the residual feed intake (RFI) of beef steers. Correlation coefficient (r) = 0.21, p-value = 0.03.

Supplementary table 3.1. Comparison of different traits between L- and H- RFI steers.

Trait	L-RFI group (efficient; n = 9)	H-RFI group (inefficient; n = 9)	p-value
RFI (kg/day)	-1.87 ± 0.34	1.95 ± 0.56	<0.001
DMI (kg/day)	8.52 ± 1.14	12.38 ± 1.25	<0.001
MEI (Mcal/day)	10.34 ± 1.38	15.02 ± 1.52	<0.001
BirthWT (kg)	43.10 ± 5.10	43.89 ± 8.43	0.973
WeanWT (kg)	543.20 ± 50.19	585.33 ± 109.60	0.398
MWT (kg)	99.71 ± 4.52	104.2 ± 9.79	0.226
EndWT (kg)	543.73 ± 41.78	575.30 ± 63.47	0.231
CWT (kg)	298.98 ± 23.54	322.24 ± 28.05	0.083
ADG (kg/day)	1.73 ± 0.41	1.78 ± 0.15	0.696

Data are Mean ± SD

Supplementary table 3.2. Differentially expressed genes (FDR<0.05) between L- and H- RFI rumen epithelium.

Ensembl ID	Gene symbol	Gene name	Fold change*	FDR adjusted p-value
ENSBTAG00000033423	*EFNA3*	Ephrin-A3	1.48	3.56E-02
ENSBTAG00000007583	*KRT14*	Keratin 14	1.47	3.91E-02
ENSBTAG00000008331	*TMEM54*	Transmembrane protein 54	1.47	1.28E-02
ENSBTAG00000005654	*TMSB10*	Thymosin beta 10	1.44	1.28E-02
ENSBTAG00000015145	*S100A11*	S100 calcium binding protein A11 (calgizzarin)	1.43	4.08E-02
ENSBTAG00000009047	*YPEL3*	Yippee-like 3 (Drosophila)	1.43	1.62E-02
ENSBTAG00000012632	*TECR*	Trans-2,3-enoyl-CoA reductase	1.43	1.02E-05
ENSBTAG00000030974	*TUBA4A*	Tubulin, alpha 4a	1.43	5.63E-04
ENSBTAG00000002631	*SCNN1A*	Sodium channel, nonvoltage-gated 1 alpha	1.41	3.60E-02
ENSBTAG00000046339	*VASN*	Vasorin	1.41	4.89E-02
ENSBTAG00000001207	*SERPINB8*	Serpin peptidase inhibitor, clade B (ovalbumin), member 8	1.41	4.00E-02
ENSBTAG00000015313	*CEACAM19*	Carcinoembryonic antigen-related cell adhesion molecule 19	1.40	1.41E-02
ENSBTAG00000007454	*RPL10*	Ribosomal protein L10	1.40	2.03E-04
ENSBTAG00000015908	*MBOAT7*	Membrane bound O-acyltransferase domain containing 7	1.39	1.91E-02
ENSBTAG00000012117	*ATP6AP1*	ATPase, H+ transporting, lysosomal accessory protein 1	1.39	2.03E-04
ENSBTAG00000000347	*RHOG*	Ras homolog gene family, member G (rho G)	1.39	1.28E-02
ENSBTAG00000025161	*AGPAT2*	1-acylglycerol-3-phosphate O-acyltransferase 2 (lysophosphatidic acid acyltransferase, beta)	1.38	2.21E-03
ENSBTAG00000018077	*LYPD3*	LY6/PLAUR domain containing 3	1.38	9.89E-04
ENSBTAG00000001350		Uncharacterized protein	1.37	1.71E-03
ENSBTAG00000018506		Uncharacterized protein	1.37	3.56E-02
ENSBTAG00000000585	*LY6G6C*	Lymphocyte antigen 6 complex, locus G6C	1.37	1.41E-02
ENSBTAG00000046100		Uncharacterized protein	1.37	2.84E-02
ENSBTAG00000015920	*TMEM147*	Transmembrane protein 147	1.35	1.28E-02
ENSBTAG00000012046	*JUNB*	Jun B proto-oncogene	1.35	4.08E-02
ENSBTAG00000025277	*ABHD17A*	Family with sequence similarity 108, member A1	1.35	2.11E-02
ENSBTAG00000009580	*SH3BGRL3*	SH3 domain binding glutamic acid-rich protein like 3	1.34	1.71E-03
ENSBTAG00000011969	*HSPB1*	Heat shock 27kDa protein 1	1.34	1.28E-02
ENSBTAG00000010626	*SH3GLB2*	SH3-domain GRB2-like endophilin B2	1.33	2.44E-02
ENSBTAG00000006241	*MAN2B1*	Mannosidase, alpha, class 2B, member 1	1.33	1.28E-02
ENSBTAG00000004875	*NAT15*	N-acetyltransferase 15 (GCN5-related)	1.32	4.86E-02
ENSBTAG00000009183	*SHISA5*	Shisa homolog 5 (Xenopus laevis)	1.32	2.49E-02

ENSBTAG00000013390	*PSMB6*	Proteasome (prosome, macropain) subunit, beta type, 6	1.32	1.41E-02
ENSBTAG00000001601	*PKM2*	Pyruvate kinase, muscle	1.30	1.28E-02
ENSBTAG00000012726	*PSMB5*	Proteasome (prosome, macropain) subunit, beta type, 5	1.30	3.48E-03
ENSBTAG00000020998	*RUVBL1*	RuvB-like 1 (E. coli)	1.30	4.00E-02
ENSBTAG00000030592	*UBL5*	Ubiquitin-like 5	1.30	4.97E-02
ENSBTAG00000010312	*MAPK1*	Mitogen-activated protein kinase 1	1.30	1.28E-02
ENSBTAG00000024091	*MALL*	Mal, T-cell differentiation protein-like	1.29	1.41E-02
ENSBTAG00000016874	*DNAJB1*	DnaJ (Hsp40) homolog, subfamily B, member 1	1.29	1.28E-02
ENSBTAG00000008172	*EGLN3*	Egl nine homolog 3 (C. elegans)	1.29	1.60E-03
ENSBTAG00000019718	*RPS15*	Ribosomal protein S15	1.29	1.85E-03
ENSBTAG00000019040	*PLBD2*	Phospholipase B domain containing 2	1.29	3.01E-02
ENSBTAG00000015406	*ZNF750*	Zinc finger protein 750	1.29	1.32E-02
ENSBTAG00000006969	*TUBB5*	Tubulin, beta; similar to tubulin, beta 5	1.28	4.02E-02
ENSBTAG00000004920	*COX8A*	Cytochrome c oxidase subunit 8A (ubiquitous)	1.28	4.61E-02
ENSBTAG00000048098	*PKP3*	Plakophilin 3	1.28	1.41E-02
ENSBTAG00000001794	*RPL36*	60S ribosomal protein L36	1.28	2.49E-02
ENSBTAG00000046350	*PKP1*	Plakophilin 1	1.27	4.08E-02
ENSBTAG00000016093	*PLP2*	Proteolipid protein 2 (colonic epithelium-enriched)	1.27	1.60E-03
ENSBTAG00000020067	*LLGL2*	Lethal giant larvae homolog 2 (Drosophila)	1.27	3.56E-02
ENSBTAG00000020560	*CLPTM1*	Cleft lip and palate associated transmembrane protein 1	1.27	1.41E-02
ENSBTAG00000004379	*ETHE1*	Ethylmalonic encephalopathy 1	1.26	3.75E-02
ENSBTAG00000019463	*SLC25A39*	Solute carrier family 25, member 39	1.26	1.91E-02
ENSBTAG00000000411	*HGS*	Hepatocyte growth factor-regulated tyrosine kinase substrate	1.26	1.28E-02
ENSBTAG00000020751	*HSF1*	Heat shock transcription factor 1	1.26	2.84E-02
ENSBTAG00000021455	*CFL1*	Cofilin 1 (non-muscle)	1.26	1.41E-02
ENSBTAG00000014872	*CAPNS1*	Calpain, small subunit 1	1.26	1.36E-02
ENSBTAG00000014553	*ATP6V0D1*	ATPase, H+ transporting, lysosomal 38kDa, V0 subunit d1	1.26	4.86E-02
ENSBTAG00000010663	*ADAM15*	ADAM metallopeptidase domain 15	1.26	3.60E-02
ENSBTAG00000016952	*PSMD5*	Proteasome (prosome, macropain) 26S subunit, non-ATPase, 5	1.26	4.07E-02
ENSBTAG00000014883	*GABARAP*	GABA(A) receptor-associated protein	1.25	3.54E-02
ENSBTAG00000018914	*RAB25*	RAB25, member RAS oncogene family	1.25	3.38E-02
ENSBTAG00000014265	*SREBF2*	Sterol regulatory element binding transcription factor 2	1.25	1.28E-02
ENSBTAG00000011904	*HCFC1*	Host cell factor C1 (VP16-accessory protein)	1.25	2.84E-02
ENSBTAG00000027075		Uncharacterized protein	1.24	4.51E-02
ENSBTAG00000015831	*RPL18A*	Similar to ribosomal protein L18a; ribosomal protein L18a	1.24	1.41E-02
ENSBTAG00000026199	*ACTB*	Actin, beta	1.24	3.13E-02

ENSBTAG00000017246; ENSBTAG00000007737	*UBC; UBA52*	Ubiquitin C; Ubiquitin A-52 residue ribosomal protein fusion product 1	1.24	1.91E-02
ENSBTAG00000016024	*MYL9*	Myosin regulatory light polypeptide 9	1.24	6.77E-03
ENSBTAG00000019782	*TPI1*	Triosephosphate isomerase 1	1.24	3.56E-02
ENSBTAG00000006495	*GNB2*	Guanine nucleotide binding protein (G protein), beta polypeptide 2	1.24	4.89E-02
ENSBTAG00000023274		Uncharacterized protein	1.23	2.32E-02
ENSBTAG00000006007	*SH3GL1*	SH3-domain GRB2-like 1	1.23	6.36E-03
ENSBTAG00000027316	*UBE2V1*	Ubiquitin-conjugating enzyme E2 variant 1	1.23	4.02E-02
ENSBTAG00000012380	*HK1*	Hexokinase 1	1.23	3.38E-02
ENSBTAG00000019851	*PPP2R1A*	Protein phosphatase 2 (formerly 2A), regulatory subunit A, alpha isoform	1.23	4.08E-02
ENSBTAG00000031875	*BANF1*	Barrier to autointegration factor 1	1.23	4.97E-02
ENSBTAG00000015434	*DSTN*	Destrin (actin depolymerizing factor)	1.22	4.86E-02
ENSBTAG00000019685	*BAG6*	BCL2-associated athanogene 6	1.22	1.28E-02
ENSBTAG00000009663	*CSDA*	Cold shock domain protein A	1.22	2.11E-02
ENSBTAG00000002381	*ZDHHC5*	Zinc finger, DHHC-type containing 5	1.21	2.44E-02
ENSBTAG00000011484	*ZDHHC3*	Zinc finger, DHHC-type containing 3	1.18	4.86E-02
ENSBTAG00000000215	*GNB1*	Guanine nucleotide binding protein (G protein), beta polypeptide 1	1.18	4.06E-02
ENSBTAG00000013362	*DNM2*	Dynamin 2	1.17	4.86E-02
ENSBTAG00000011488	*PRPF8*	PRP8 pre-mRNA processing factor 8 homolog (S. cerevisiae)	1.16	2.50E-02
ENSBTAG00000016080	*VPS13D*	Vacuolar protein sorting 13 homolog D (S. cerevisiae)	0.85	2.11E-02
ENSBTAG00000009780	*GTF2I*	General transcription factor II, i	0.85	4.86E-02
ENSBTAG00000009541	*SUCLG2*	Succinate-CoA ligase, GDP-forming, beta subunit	0.84	4.86E-02
ENSBTAG00000021209	*UBR5*	Ubiquitin protein ligase E3 component n-recognin 5	0.83	3.60E-02
ENSBTAG00000008862	*GOLGB1*	Golgin B1	0.82	2.84E-02
ENSBTAG00000006940	*USP48*	Ubiquitin specific peptidase 48	0.81	4.86E-02
ENSBTAG00000009061	*FAR1*	Fatty acyl CoA reductase 1	0.80	4.86E-02
ENSBTAG00000020914	*CPNE8*	Copine VIII	0.79	4.06E-02
ENSBTAG00000016038	*GCC2*	GRIP and coiled-coil domain containing 2	0.79	2.84E-02
ENSBTAG00000003697	*TARDBP*	TAR DNA binding protein	0.78	4.80E-02
ENSBTAG00000020233	*CCDC186*	Coiled-coil domain containing 186	0.78	4.86E-02
ENSBTAG00000005443	*MIER1*	Mesoderm induction early response 1 homolog (Xenopus laevis)	0.78	2.49E-02
ENSBTAG00000038488	*TMSB4*	Thymosin beta 4, X-linked	0.77	1.60E-03
ENSBTAG00000027569	*APBB2*	Amyloid beta (A4) precursor protein-binding, family B, member 2	0.77	4.00E-02
ENSBTAG00000019500	*CNIH1*	Cornichon homolog (Drosophila)	0.76	2.59E-02
ENSBTAG00000001485	*PPIP5K2*	Diphosphoinositol pentakisphosphate kinase 2	0.76	1.41E-02
ENSBTAG00000047537	*CCAR1*	Cell division and apoptosis regulator 1	0.75	2.44E-02
ENSBTAG00000015612	*UTP6*	Small subunit processome component	0.74	4.66E-02

ENSBTAG00000047029		Uncharacterized protein	0.73	4.86E-02
ENSBTAG00000014044	*VEZT*	Vezatin, adherens junctions transmembrane protein	0.73	4.18E-02
ENSBTAG00000014099	*YTHDC2*	YTH domain containing 2	0.73	2.84E-02
ENSBTAG00000011187	*FAM13A*	Family with sequence similarity 13, member A1	0.73	4.36E-02
ENSBTAG00000014469	*NBEAL1*	Neurobeachin-like 1	0.72	6.05E-03
ENSBTAG00000003064	*GCFC*	GC-rich sequence DNA-binding factor homolog	0.72	4.86E-02
ENSBTAG00000013982	*UACA*	Uveal autoantigen with coiled-coil domains and ankyrin repeats	0.72	2.11E-02
ENSBTAG00000037440		Uncharacterized protein	0.71	4.18E-02
ENSBTAG00000027728	*NUDT12*	Nudix (nucleoside diphosphate linked moiety X)-type motif 12	0.71	1.28E-02
ENSBTAG00000026233		Uncharacterized protein	0.70	2.11E-02
ENSBTAG00000034580	*TMSB4*	Thymosin beta-4 Hematopoietic system regulatory peptide	0.70	1.41E-02
ENSBTAG00000045772		Uncharacterized protein	0.69	1.37E-02
ENSBTAG00000016932	*SENP7*	SUMO1/sentrin specific peptidase 7	0.68	1.41E-02
ENSBTAG00000009035	*CENPE*	Centromere protein E, 312kDa	0.68	2.84E-02
ENSBTAG00000006255	*MDM4*	Mdm4 p53 binding protein homolog (mouse)	0.68	2.59E-02
ENSBTAG00000042484	*SNORD22*	Small nucleolar RNA SNORD22	0.67	4.00E-02
ENSBTAG00000000782	*KDR*	Kinase insert domain receptor (a type III receptor tyrosine kinase)	0.65	2.84E-02
ENSBTAG00000005445	*SLC35D2*	Solute carrier family 35 (UDP-glucuronic acid/UDP-N-acetylgalactosamine dual transporter), member D1	0.65	5.63E-04
ENSBTAG00000048293	*U2*	U2 spliceosomal RNA	0.64	2.84E-02

*Fold change is gene expression in L-RFI relative to H-RFI

CHAPTER 4. THE RELATIVE ACTIVITY OF RUMEN EPITHELIAL BACTERIA AND ARCHAEA IN BEEF CATTLE DIVERGENT IN RESIDUAL FEED INTAKE

4.0 Introduction

Ruminant animals, such as cattle, contain a large and diverse community of microorganisms within the rumen that consist of bacteria, archaea, protozoa, and fungi (Kamra, 2005). The rumen microbes are often classified into three populations based on their localization. There are microbes associated with the rumen fluid, feed particles, and the rumen epithelial wall (McCowan et al., 1978; Olubobokun and Craig, 1990). A major function of rumen bacteria is in feed degradation and fermentation, which generates a large supply of energetic substrates for the host to utilize (Bergman, 1990). The waste products of fermentation, such as hydrogen and carbon dioxide, are converted to methane (CH_4) by methanogenic archaea that belong to the phylum *Euryarchaeota* (Liu and Whitman, 2008; Morgavi et al., 2010). It has been found that the most abundant rumen methanogens, as characterized by 16S rRNA gene sequencing, are from the order *Methanobacteriales* and the genus *Methanobrevibacter* (Pei et al., 2010; Seedorf et al., 2015). CH_4 emission, however, represents a dietary loss of energy (Johnson and Ward, 1996) and is a major contributor to global warming (Lelieveld et al., 1998).

Differences in the composition and activity of the rumen microorganisms may contribute to variation in host feed efficiency through their influence on feed digestion, fermentation, and CH_4 production. The feed efficiency of an individual can be measured by residual feed intake (RFI), which is calculated as the difference between actual feed intake and expected feed requirements for growth and maintenance (Basarab et al., 2003). Animals with low RFI (L-RFI) are considered feed efficient while those with high RFI (H-RFI) are deemed feed inefficient. Feed efficient cattle produce approximately 25% less CH_4 than inefficient cattle (Hegarty et al.,

2007) and consume 3.77 kg less feed per day for similar growth and body weight (Basarab et al., 2003). Studies of methanogens within the rumen fluid of cattle differing in feed efficiency, have found that the abundance of total methanogens were not different between RFI groups (Zhou et al., 2009; Zhou et al., 2010). However, the feed inefficient individuals had a more diverse methanogenic community and greater abundance of *Methanosphaera stadtmanae* and *Methanobrevibacter* sp. Strain AbM4 compared to efficient animals (Zhou et al., 2009). When the ruminal fluid bacterial community was assessed, it was discovered that the abundance of particular bacterial phylotypes are associated with feed efficiency (Hernandez-Sanabria et al., 2012).

To date, there have been no studies examining the rumen epithelial attached microbes (epimural community) in relation to feed efficiency. It has been found that the predominant bacteria identified on the epithelium belong to the phylum *Firmicutes* (Li et al., 2012). Characterization of epimural bacteria found they have specific roles in the rumen such as mucosal protection, urea hydrolysis, epithelial recycling, and oxygen scavenging (Holovska et al., 2002; Cheng and Wallace, 1979; McCowan et al., 1978; Cheng et al., 1979). The hydrolysis of urea from the rumen wall by ureolytic bacteria provides ammonia for microbial protein synthesis, which is a major source of protein for the host. Oxygen scavenging by facultative anaerobes on the epithelium removes oxygen, thereby protecting obligate anaerobes and maintaining optimal fermentation conditions.

The objective of this study was to investigate the differences in activity of rumen epithelial attached bacteria and archaea between low and high feed efficient beef cattle. The relative abundance of bacterial and archaeal 16S rRNA transcripts obtained from RNA-sequencing (RNA-seq) was used to infer activity of the epimural microbial community. Because the phylum *Euryarcheota* contains the methanogens, we predicted archaea from this phylum

would have the highest activity of the archaea on the rumen epithelium; specifically, the highly abundant *Methanobrevibacter* archaea would be the most active archaea on the epithelium. We hypothesized that the activity of CH_4 producing archaea, such as *Methanobrevibacter*, would be lowest on the rumen epithelium of L-RFI (feed efficient) cattle because they are known to produce less CH_4 than H-RFI (feed inefficient) cattle. For epithelial bacteria, we predicted activity from the phylum *Firmicutes* would be highest in both L- and H- RFI animals due to their high abundance on the epithelium. Additionally, the L-RFI animals are predicted to have the greatest activity of ureolytic and oxygen scavenging bacteria, which possibly contributes to high feed efficiency.

4.1 Materials and Methods

4.1.1 Animals and rumen tissue collection

All experimental procedures were approved by the University of Alberta Animal Care and Use Committee for Livestock (Moore-2006-55) and animals were raised in accordance with the Canadian Council of Animal Care guidelines (CCAC, 1993). At 10 months old, 175 Hereford x Aberdeen Angus hybrid steers at the University of Alberta Roy Berg Kinsella Research Station (Alberta, Canada) were placed under feedlot conditions. The growing diet was fed for 90 days and consisted of 74% oats, 20% hay, and 6% feedlot supplement (32% CP beef supplement containing Rumensin (400 mg/kg) and 1.5% canola oil). Then, steers had a one week adaptation period before starting a 90 day period on a finishing diet containing 56.7% barley, 28.3% oats, 10% alfalfa pellets, and 5% feedlot supplement (32% CP beef supplement containing Rumensin (400 mg/kg) and 1.5% canola oil). Feed intake data was collected throughout the feeding trial using the GrowSafe automated feeding system (GrowSafe Systems Ltd., Airdrie, Alberta, Canada) and RFI was calculated for each feeding period as described by Nkrumah et al. (2006).

The RFI after the high-energy, finishing diet was used to classify steers as L-RFI (feed efficient; RFI < -0.5), medium RFI (M-RFI; -0.5 ≤ RFI ≤ 0.5), or H-RFI (feed inefficient; RFI > 0.5).

Steers were slaughtered after the feeding trial and rumen tissue (4-cm^2) was collected from the central region of the ventral sac. The tissue was placed in RNAlater solution (Invitrogen, Carlsbad, CA) and stored at -80°C until further processing. RNA extraction and sequencing was performed on the rumen epithelium from nine extreme L-RFI (RFI = -1.4 to -2.33 kg/day) and nine extreme H-RFI (RFI = 1.32 to 3.23 kg/day) steers as described in Chapter 3.

4.1.2 RNA extraction and sequencing

Papillae (~80 mg) were removed from the rumen tissue using scissors and scalpel. Then, the mirVana kit (Ambion, Austin, TX) was used to isolate total RNA from the papillae according to the manufacturer's instructions. The RNA integrity, concentration, and purity of total RNA were measured using the Agilent 2100 Bioanalyzer (Agilent Technologies, Santa Clara, CA) and Nanodrop 2000c spectrophotometer (Thermo Scientific, Wilmington, DE).

Next, total RNA samples (n=18) were prepared for RNA-seq by creating cDNA libraries from 100 ng of total RNA following the protocol of the TruSeq RNA Sample Preparation v2 kit (Illumina, San Diego, CA). Polymerase chain reaction (15 cycles) was used to amplify libraries, which were then validated and quantified with the Agilent 2200 TapeStation (Agilent Technologies) and Qubit fluorometer (Invitrogen, Carlsbad, CA), respectively. Lastly, the RNA libraries were sequenced on the Illumina HiSeq 2000 system at the McGill University and Genome Quebec Innovation Centre (Quebec, Canada) to obtain high quality, 100 base pair (bp), paired-end reads (Average quality score ≥ 33). The raw sequencing data have been deposited at publicly available NCBI's Gene Expression Omnibus Database

(http://www.ncbi.nlm.nih.gov/geo/). The data are accessible through GEO Series accession number GSE74394 (http://www.ncbi.nlm.nih.gov/geo/query/acc.cgi?acc=GSE74394).

4.1.3 Quantification and identification of bacterial and archaeal 16S rRNA transcripts

High quality RNA-seq reads (i.e. transcripts) were first aligned to the bovine reference genome, UMD3.1 (Ensembl v83.31) using the software packages TopHat2 (v2.0.9; Kim et al., 2013) and Bowtie2 (v2.1.0; Langmead and Salzberg, 2012). Sequencing reads that could not be aligned to the bovine genome were input to SortMeRNA (v1.99-beta; Kopylova et al., 2012) to obtain reads encoding bacteria and archaea 16S rRNA. The 16S rRNA paired reads were then assembled into contigs and the Mothur program (v1.31.2; Schloss et al., 2009) was used to align contigs to bacteria and archaea 16S rRNA databases in order to identify and quantify the transcripts. The contigs were aligned to the V1-V3 variable region of the 16S rRNA gene using the Greengenes database (v13.5.99; DeSantis et al., 2006) for bacteria and contigs were also aligned to the V6-V8 region using a database compiled by Janssen and Kirs (2008) for archaea. Bacteria were only classified down to the family level, while archaea were classified to the genus level because the contigs (96-200 bp) were too short to be reliably classified at the lower taxonomic levels. The bacteria and archaea transcripts were identified at 100% similarity with the database. Three animals from each of the RFI groups were removed from further analyses due to their low number of transcripts detected for bacteria and archaea. The proportion of 16S rRNA transcripts for every bacterial and archaeal phylotype was determined for every sample and the average proportion for each phylotype was calculated for each RFI group. Only phylotypes with an average abundance of 16S rRNA transcripts $\geq 0.5\%$ in at least one RFI group are described in this study. An unpaired t-test in the SAS statistical program (v9.2; SAS Institute

Inc., Cary, NC) was used to determine statistical significance ($p<0.05$) between RFI groups in the relative abundance of 16S rRNA transcripts for each phylotype.

4.2 Results

4.2.1 Identification and quantification of archaeal 16S rRNA transcripts

The total number of archaeal 16S rRNA transcripts obtained per epithelial sample through RNA-seq was 31,999 ± 20,416 (mean ± SD). At the phylum level, *Euryarchaeota* and an unclassified phylum were detected from the transcripts (Figure 4.1). *Euryarchaeota* contributed to 81.3% and 84.6% of the relative abundance of archaeal 16S rRNA transcripts from the epithelial tissue of the L- and H- RFI groups, respectively. The archaeal genera consisted of *Methanopyrus*, *Methanobrevibacter*, *Methanosarcina*, unclassified genera from the order *Methanobacteriales*, unclassified genera from the phylum *Euryarchaeota*, and genera that could not be classified at any taxonomic level below kingdom archaea (Figure 4.2). The majority of the archaeal 16S rRNA transcripts were from genera that were unclassified *Euryarchaeota.* They contributed 73.6% and 72.4% of total archaeal transcripts from the L- and H- RFI epitheliums, respectively. There was also a high relative abundance of transcripts from the archaeal genera that could not be classified below kingdom and from *Methanobrevibacter.* The unclassified archaea had 18.7% relative transcript abundance on the L-RFI epithelium and 15.4% on the H-RFI epithelium. *Methanobrevibacter* relative transcript abundance was lower on the L-RFI epithelium (5.8%) compared to on the H-RFI epithelium (9.3%). However, there was no significant difference found between the RFI groups in the relative abundance of 16S rRNA transcripts for any of the archaeal phylotypes ($p>0.05$).

4.2.2 Identification and quantification of bacterial 16S rRNA transcripts

From RNA-seq, there were 59,166 ± 35,148 (mean ± SD) total number of bacterial 16S rRNA transcripts per epithelial sample. Of the phyla that could be classified, the *Proteobacteria* phylum had the most abundant 16S rRNA transcripts in both RFI groups followed by *Firmicutes*, *Bacteroidetes*, and *Synergistetes* (Figure 4.3). There was a higher relative abundance of transcripts from *Proteobacteria* on the L-RFI epithelium (54.5%) than on the H-RFI epithelium (43.3%). For each phylum, however, there was no significant difference in the relative abundance of transcripts between the RFI groups ($p>0.05$). Additionally, bacterial families were identified and included *Campylobacteraceae*, *Comamonadaceae*, *Desulfobulbaceae*, *Dethiosulfovibrionaceae*, *Lachnospiraceae*, *Mogibacteriaceae*, *Neisseriaceae*, *Prevotellaceae*, *Ruminococcaceae*, *Succinivibrionaceae*, *Veillonellaceae*, unclassified *Bacteroidetes*, unclassified *Firmicutes*, unclassified *Proteobacteria*, and families that could not be classified below kingdom bacteria (Figure 4.4). *Succinivibrionaceae* had the highest relative abundance of bacterial transcripts on both the L-RFI (28.7%) and H-RFI (33.9%) epithelium. Although *Succinivibrionaceae* transcripts were greater in the H-RFI group, it was not statistically significant ($p>0.05$). Of the bacterial families, *Campylobacteraceae* and *Neisseriaceae* had significantly greater transcripts on the L-RFI epithelium ($p<0.05$) than on the H-RFI epithelium. The L-RFI group had 5.8% of transcripts from *Campylobacteraceae*, while the H-RFI group had 2.4%. *Neisseriaceae* contributed 10.8% and 1.0% of total transcripts on the L- and H- RFI epithelium, respectively.

4.3 Discussion

There have been few studies examining the association between the rumen microbial community and feed efficiency in cattle. No knowledge about the composition and activity of

epithelial attached microbes in relation to feed efficiency currently exist. Therefore, in our study we used RNA-seq to investigate the relative activity of rumen epithelial attached bacteria and archaea in L- and H- RFI beef steers.

For the epimural archaea, we found there was activity from the phylum *Euryarchaeota* as well as from an unclassified phylum. However, the majority of the activity was from archaea belonging to *Euryarchaeota*, which accounted for 81.3% and 84.6% of the total archaeal activity on the L- and H- RFI epithelium, respectively. This was expected, as methanogens are classified in *Euryarchaeota* and are responsible for methanogenesis, a major process in the rumen (Liu and Whitman, 2008; Morgavi et al., 2010). At the genus level, a large proportion of the archaeal activity (~70%) was from unclassified genera from *Euryarchaeota*. This was contrary to our hypothesis that archaea from the *Methanobrevibacter* genus would be the most active based on their high abundance on the epithelium. *Methanobrevibacter* contributed to less than 10% of the archaeal activity although they are the most predominant genus on the epithelium (Pei et al., 2010). This suggests that while *Methanobrevibacter* are highly abundant, they are not the most transcriptionally active archaeal genus on the epithelium. Because methanogens from unclassified genera of *Euryarchaeota* are highly active on the epithelium, it indicates that they may be responsible for a majority of the CH_4 production on the epithelium and that methanogenesis is a major role of epimural archaea. However, their abundance is low compared to their activity. It has been reported that only 25.5% of epithelial associated methanogens are unidentified *Euryarchaeota* (Pei et al., 2010). Further studies need to be conducted to identify the unclassified *Euryarchaeota* to determine which methanogenic genus is the most active on the epithelium. Additionally, we found that archaea that could not be classified below kingdom level (unclassified archaea) also seem to be quite active on the epithelium (15.4% - 18.7% relative activity), which may have roles other than in methanogenesis. This is the first study detecting a

phylum other than *Euryarchaeota* and *Crenarcheota* in the rumen (Shin et al., 2004; Janssen and Kirs, 2008). Future work is needed to identify the unclassified archaeal phylum to determine how they contribute to rumen function. Moreover, we had predicted there would be lower methanogen activity on the L-RFI epithelium since L-RFI steers produce less CH_4 than H-RFI steers, however, we found no significant difference between the L- and H- RFI epithelium in the relative activity of any of the archaeal phylotypes. This suggests that the difference in CH_4 production between the RFI groups may be predominantly due to differences in the activity of the methanogens in the rumen content. Therefore, studying the activity of methanogens associated with rumen content may be a superior indicator of methanogenesis.

We hypothesized that the activity of rumen epithelial bacteria from the phylum *Firmicutes* would be the highest since *Firmicutes* was identified as the predominant bacterial phylum on the epithelium at DNA level (Li et al., 2012). However, the bacterial phylum with the greatest activity on the rumen epithelium was *Proteobacteria*, followed by *Firmicutes* and *Bacteroidetes*. This suggests that although *Firmicutes* had the highest abundance on the epithelium at DNA level, it is not necessary that they had the highest activity (at RNA level). Others have also found that the activity of *Proteobacteria* in the rumen was higher than *Firmicutes* even though *Proteobacteria* had lower abundance (Kang et al., 2013). We found that the most active bacterial family on the rumen epithelium was *Succinivibrionaceae*, which belong to the *Proteobacteria* phylum. The *Succinivibrionaceae* family contains the genera *Anerobiospirillum*, *Ruminobacter*, *Succinimonas*, and *Succinivibrio* (Stackebrant and Hespell, 2006). It is known that *Succinivibrio dextrinosolvens* has urease and other nitrogen assimilation enzymes such as glutamine synthetase and glutamate (Patterson and Hespell, 1985). Although the *Succinivibrionaceae* family contains ureolytic species to convert urea to ammonia, the activity of this family does not significantly differ between RFI groups. However, analysis at the

species level is needed to determine the difference in activity of urease producers between L- and H- RFI cattle. While there was no significant difference in activity of *Succinivibrionaceae* between RFI groups, we found significantly higher ($p<0.05$) activity from the families *Campylobacteraceae* and *Neisseriaceae* on the L-RFI epithelium. Both *Campylobacteraceae* and *Neisseriaceae* are *Proteobacteria*. *Campylobacteraceae* contains the genera *Campylobacter* and *Arcobacter*, which are known to colonize mucosal surfaces (Lastovica et al., 2014). Most *Campylobacter* species have oxidase activity that catalyzes the reduction of oxygen to water (Lastovica et al., 2014). *Neisseriaceae*, which contains the genus *Neisseria*, are also known to colonize mucosal surfaces and have oxidase activity (Jurtshuk and Milligan, 1974). Because the *Campylobacteraceae* and *Neisseriaceae* families have oxygen scavenging function and have significantly higher activity in L-RFI steers, it suggests that L-RFI animals have better oxygen removal from the rumen and maintenance of the anaerobic condition for fermentation. Optimal fermentation conditions result in effective feed fermentation and may contribute to high feed efficiency by providing an increased supply of energetic substrates for the host to utilize as energy.

In summary, we found that approximately 70% of the archaeal activity on the rumen epithelium was from unclassified genera from phylum *Euryarchaeota*, which emphasizes the need for further studies to classify unknown rumen methanogens. Our study showed that the relative activity of archaeal phylotypes on the epithelium was not significantly different between L- and H- RFI steers, which suggests that rumen epithelial attached methanogens do not contribute to differences in CH_4 production and variation in feed efficiency. The most active epithelial attached bacteria were from the phylum *Proteobacteria*, which was unexpected as *Proteobacteria* abundance is not as high as *Firmicutes* on the epithelium (Li et al., 2012). There was no significant difference between RFI groups in the activity of ureolytic bacterial

phylotypes; however, we found that the families *Campylobacteraceae* and *Neisseriaceae*, which contain oxygen scavenging bacteria were significantly more active on the L-RFI epithelium. Therefore, L-RFI steers may have more optimal rumen fermentation conditions for feed fermentation and generation of energetic substrates for energy production by the host.

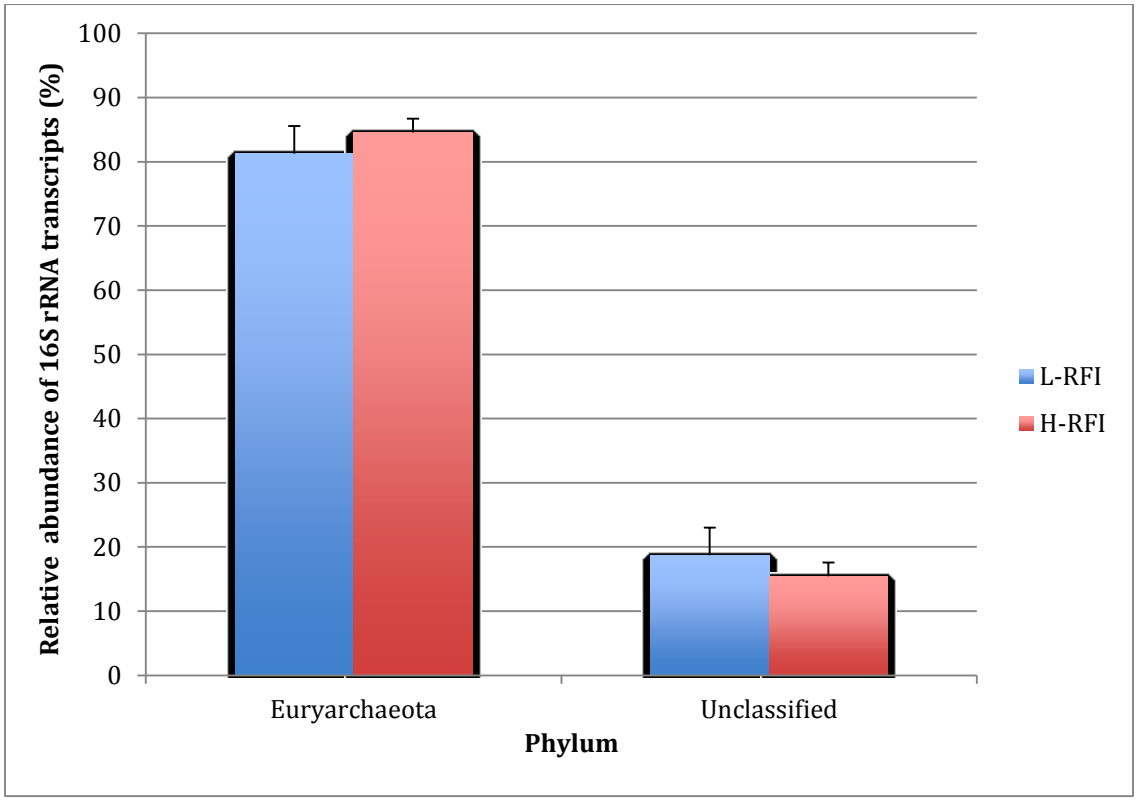

Figure 4.1. The relative abundance of 16S rRNA transcripts belonging to each archaeal phylum on the rumen epithelium of L-RFI (n=6; blue) and H-RFI (n=6; red) beef steers. Relative abundance is given as a percentage and data are presented as mean ± SEM.

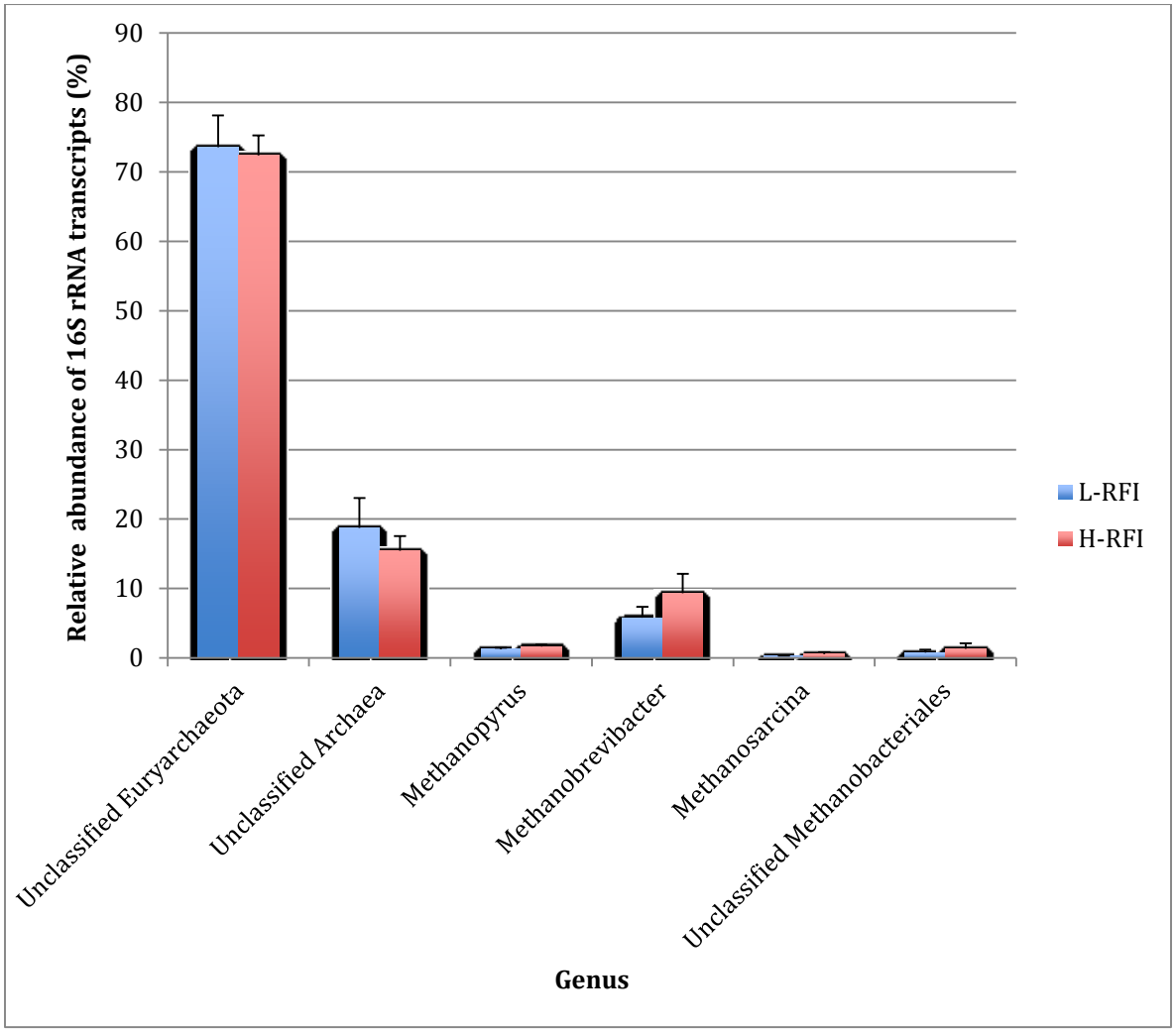

Figure 4.2. The relative abundance of 16S rRNA transcripts belonging to each archaeal genus on the rumen epithelium of L-RFI (n=6; blue) and H-RFI (n=6; red) beef steers. Relative abundance is given as a percentage and data are presented as mean ± SEM.

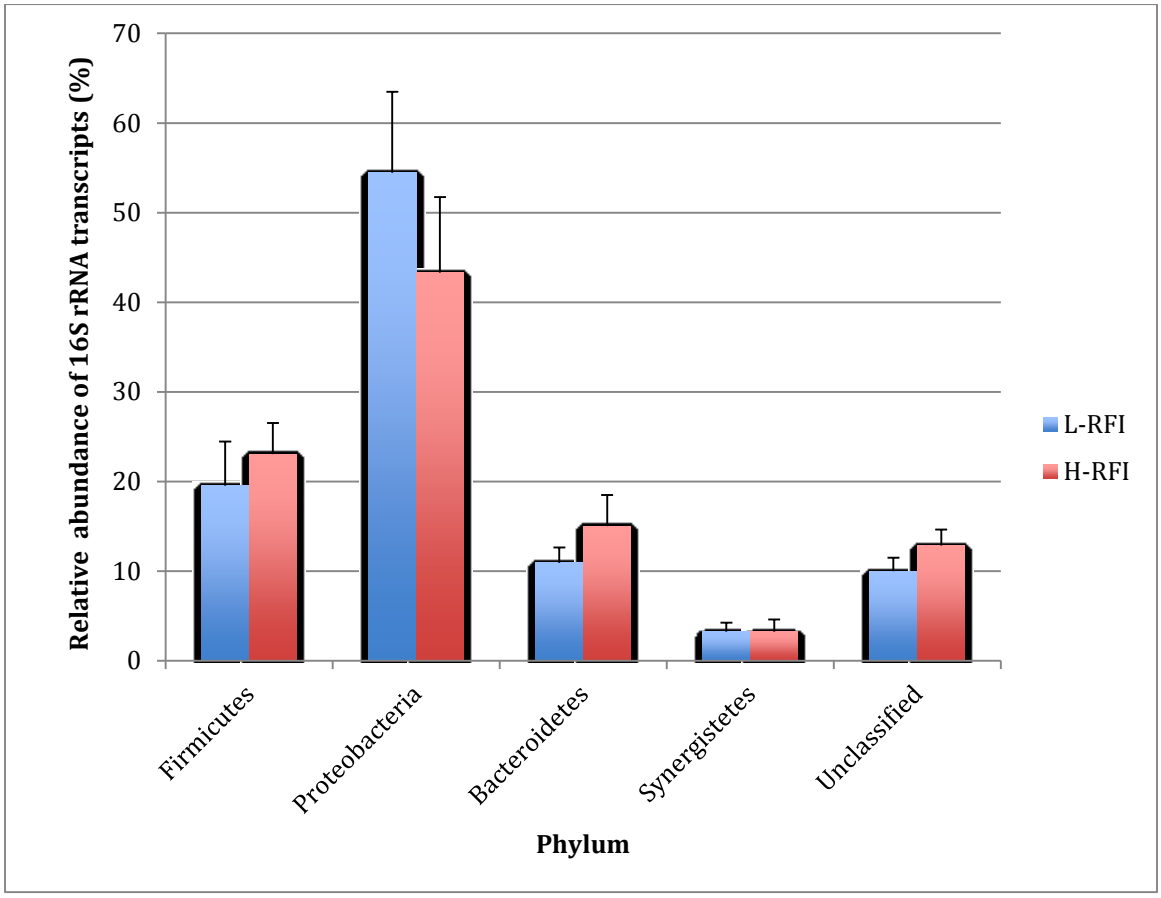

Figure 4.3. The relative abundance of 16S rRNA transcripts belonging to each bacterial phylum on the rumen epithelium of L-RFI (n=6; blue) and H-RFI (n=6; red) beef steers. Relative abundance is given as a percentage and data are presented as mean ± SEM.

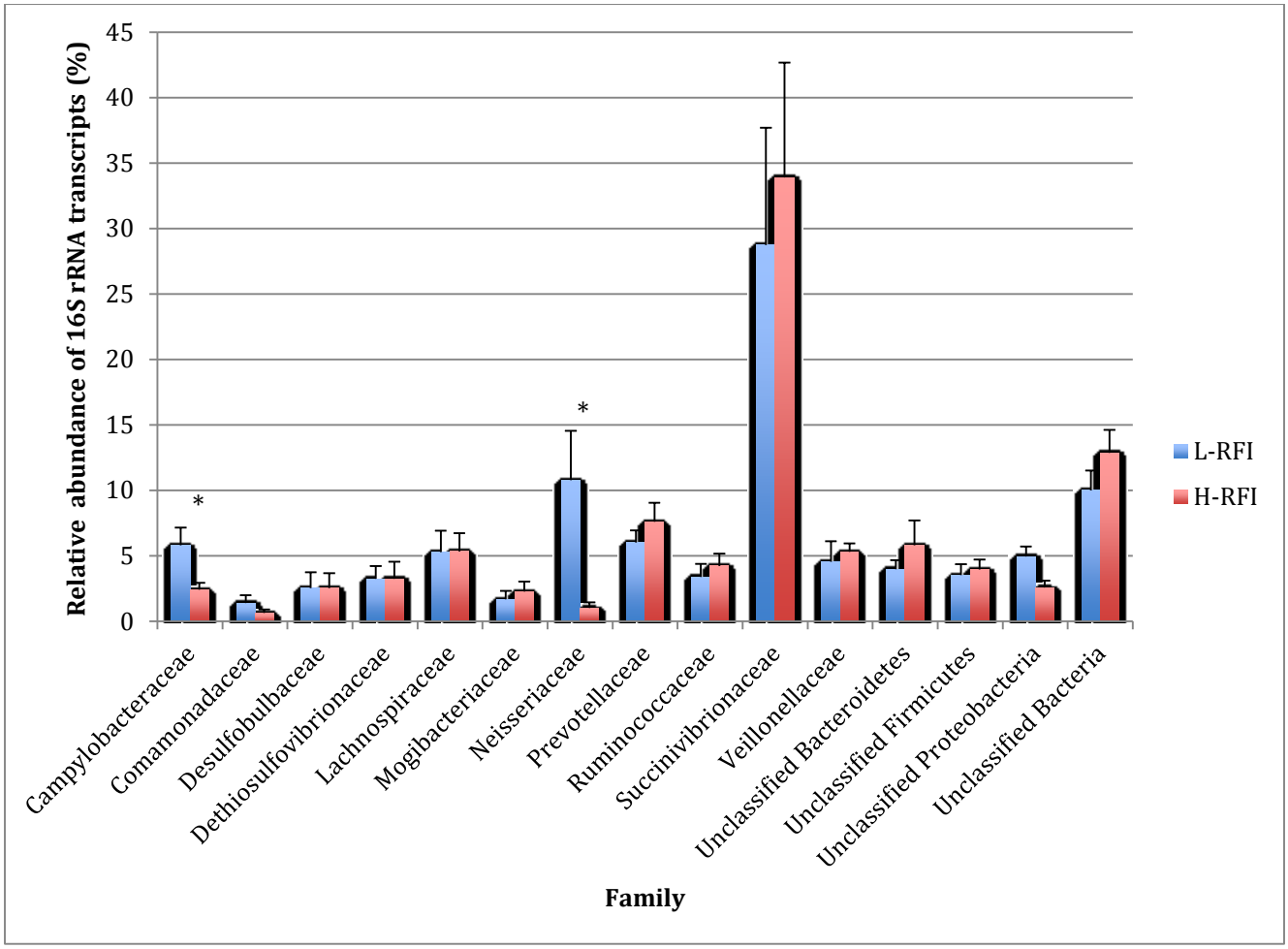

Figure 4.4. The relative abundance of 16S rRNA transcripts belonging to each bacterial family on the rumen epithelium of L-RFI (n=6; blue) and H-RFI (n=6; red) beef steers. Relative abundance is given as a percentage and data are presented as mean ± SEM.

CHAPTER 5. GENERAL DISCUSSION

There has been great interest in improving the feed efficiency of cattle for sustainable beef production, increased profitability and a reduction in environmental pollution. Residual feed intake (RFI) is an optimal feed efficiency trait to select for due to its independence from growth traits. For improvement to occur through genetic selection, we would need to increase our understanding of the molecular mechanisms underlying physiological processes that affect RFI. Our first study examined whether host gene expression in the rumen epithelium contributes to variation in feed efficiency. We predicted there would be a difference between low RFI (L-RFI) and high RFI (H-RFI) steers in the expression of genes involved in the absorption and metabolism of short-chain fatty acids (SCFAs), which are a major energy source for cattle. In relation to absorption, our results showed no difference between RFI groups in the expression of genes encoding SCFA transporters. However, feed efficient (L-RFI) steers had increased expression of genes involved in tissue morphogenesis that may increase the paracellular permeability of the epithelium for the simple diffusion of nutrients, such as SCFAs. For example, the L-RFI epithelium had up-regulation of genes involved in regulating intercellular adhesion, cell migration, cell and protein turnover, and cytoskeletal organization. Other studies have observed dynamic changes in the rumen epithelium as a result of high SCFA concentrations (Steele et al., 2011), which suggests that L-RFI animals have a greater ruminal supply of SCFAs. Although the L-RFI epithelium had increased expression of genes involved in processes that may increase simple diffusion of nutrients, we did not observe differences between the L- and H- RFI epithelium in the expression of genes involved in the metabolism of SCFAs. Further studies to investigate the proteins that are associated with metabolism, transporters, and permeability are necessary to confirm the findings. Moreover, differences in SCFA metabolism may exist in other tissues, such as the liver; however, no studies to date have examined the differences in SCFA

metabolism between the RFI groups in other tissues. This illustrates the importance in examining the gene expression profile within different tissues to understand how they contribute to variation in feed efficiency. The L-RFI rumen epithelium, however, may have a greater glycolytic potential and energy generation due to increased expression of genes involved in glycolysis, oxidative phosphorylation, and acetylation. Because we found increased expression of oxidative phosphorylation genes and reduced mitochondrial copy numbers in the L-RFI rumen, we believe that they have more efficient mitochondria than H-RFI cattle. Future studies are needed to examine the activity and efficiency of mitochondria in the rumen to determine whether L-RFI animals have greater energy production due to increased mitochondrial efficiency and activity. We propose that an increase in local energy production is required for the increased tissue morphogenesis occurring in the L-RFI rumen. Further studies are needed to determine whether there are truly differences in tissue morphogenesis between the rumen epithelial tissues of cattle differing in RFI by examining tissue morphology directly using techniques such as electron microscopy and histology. Overall, host gene expression in the rumen epithelium may contribute to variation in feed efficiency by affecting the simple diffusion of nutrients. Feed efficient steers have up-regulation of genes that may increase the simple diffusion of SCFAs. A greater supply of SCFAs may enter portal circulation to the liver and peripheral tissues for whole-body energy generation because no increase in SCFA metabolism was observed in the L-RFI epithelium. Multiple genes in various biological processes and tissues are likely involved in influencing feed efficiency. Therefore, a combination of genes from many processes and tissues are needed to generate a selection index in order to improve RFI.

Any factors that impact feed intake or utilization may contribute to variation in feed efficiency. To improve RFI, we have to consider factors other than host genetics. For example, the rumen microorganisms are vital to feed fermentation, which produce nutrients for the host

and methane (CH_4) (Bergman et al., 1990). Differences in the microbial population in the rumen content have been associated with variation in RFI (Guan et al., 2008; Zhou et al., 2009; Hernandez-Sanabria et al., 2010; Zhou et al., 2010; Hernandez-Sanabria et al., 2012). However, the influence of the microbial community attached to the rumen epithelium on feed efficiency has not been studied before. The epithelial-attached microbes are important because they participate in feed digestion, fermentation, and have other functions that may be important to feed efficiency (Zhang et al., 2007). These additional functions include protein recycling, ureolysis, and oxygen scavenging (McCowan et al., 1978; Cheng et al., 1979). Our second study examined the differences in the activity of rumen epithelial attached archaea and bacteria between beef cattle differing in RFI. Methanogenic archaea are slow-growing organisms that are capable of colonizing the epithelium in order to avoid passage from the rumen (Janssen and Kirs, 2008; Khelaifia et al., 2013). They mainly act as a hydrogen sink by utilizing hydrogen, thereby maintaining an optimal fermentation condition in the rumen because hydrogen inhibits the complete oxidation of substrates (Moss et al., 2000). Little is known about the mechanisms in which methanogens attach to the epithelium, however studies have found they may adhere by uncharacterized adhesion-like proteins (Samuel et al., 2007; Leahy et al., 2010). No difference was found between RFI groups in the activity of epithelial archaea, suggesting that lower CH_4 production in L-RFI animals may be mainly due to differences in the activity of CH_4-producing archaea in the rumen content. To date, there have been no studies examining the activity of rumen content associated archaea in relation to feed efficiency. Although L-RFI animals have been reported to produce less CH_4, the CH_4 was not measured for the animals used in this study. While there was no difference in the activity of archaeal phylotypes between RFI groups, the L-RFI epithelium showed greater activity of the bacterial families, *Campylobacteraceae* and *Neisseriaceae*, which contain oxygen scavengers. Future studies are necessary to identify the

genera and species within these two identified families to further elucidate their roles in relation with feed efficiency. Regardless, based on our results we speculate that the rumen epithelial attached bacteria may contribute to high feed efficiency by providing more optimal fermentation conditions for obligate anaerobes.

There were several limitations of the research conducted for this thesis. The epithelial tissue used in the research was obtained from only one location within the rumen. Pooling epithelial samples from multiple locations in the rumen is recommended to provide a better representation of the host transcriptome and abundance of microbial 16s rRNA transcripts. Another limitation was that the epithelial tissue was acquired from animals only after slaughter. The transcriptome and activity of microbes within animals may vary throughout their life. Therefore, it would be optimal to obtain epithelial samples from live animals through biopsy at various time points throughout the day and at different ages of the animal. An additional limitation was that the concentration and absorption of ruminal SCFAs were not measured. Future work is needed to determine whether feed efficient steers truly have a greater supply of SCFAs and increased simple diffusion of SCFAs through the rumen wall. The use of the Illumina HiSeq 2000 system for RNA-seq provided another limitation because the sequencing reads generated were too short to reliably classify archaea below genus level and bacteria below family level. A long-read sequencing technology is therefore required to classify microbial phylotypes at lower taxonomic levels. However, the current long-read sequencing technologies have low yield and accuracy compared to short-read technologies (Jänes et al., 2015). Although the transcriptional activity of the microbes was measured, the functional activity of the microbes was not determined. It is important to understand how the functional activity of microbes is associated with feed efficiency in order to alter microbial activity or composition to improve cattle feed efficiency.

In conclusion, host gene expression in the rumen epithelium and certain bacterial phylotypes associated with the epithelium impact the feed efficiency of beef cattle. Further work is needed to identify all the factors, mechanisms, and genes responsible for variation in feed efficiency in order to improve selection without adversely affecting other economically important traits. Understanding how genes are associated with traits may also provide ideas on how to genetically modify traits. Furthermore, modification of the rumen microbial community may improve feed efficiency because rumen microbes impact feed digestion and fermentation.

LITERATURE CITED

Akin DE, Borneman WS. Role of rumen fungi in fiber degradation. J Dairy Sci. 1990; 73(10):3023-3032.

Alberts B, Johnson A, Lewis J, et al. Molecular biology of the cell. 4th edition. The Mitochondrion. New York: Garland Science; 2002.

Alston JM, Pardey PG. Agriculture in the global economy. J Econ Perspect. 2014; 28(1):121-146.

Anders S, Pyl PT, Huber W. HTSeq – a Python framework to work with high-throughput sequencing data. Bioinform. 2015; 31(2):166-169.

Andersen CL, Ledet-Jensen J, Ørntoft T. Normalization of real-time quantitative RT-PCR data: a model based variance estimation approach to identify genes suited for normalization applied to bladder and colon cancer datasets. Cancer Res. 2004; 64:5245-5250.

Apodaca G. Endocytic traffic in polarized epithelial cells: role of the actin and microtubule cytoskeleton. Traffic. 2001; 2:149-159.

Archer JA, Bergh L. Duration of performance tests for growth rate, feed intake and feed efficiency in four biological types of beef cattle. Livest Prod Sci. 2000; 65(1):47-55.

Argyle JL, Baldwin RL. Effects of amino acids and peptides on rumen microbial growth yields. J Dairy Sci.1989; 72:2017-2027.

Arthur PF, Archer JA, Johnston DJ, Herd RM, Richardson EC, Parnell PF. Genetic and phenotypic variance and covariance components for feed intake, feed efficiency, and other postweaning traits in Angus cattle. J Anim Sci. 2001; 79:2805-2811.

Arthur JP, Herd RM. Residual feed intake in beef cattle. R Bras Zootec. 2008; 37:269-279.

Aschenbach JR, Bilk S, Tadesse G, Stumpff F, Gabel G. Bicarbonate-dependent and bicarbonate-independent mechanisms contribute to nondiffusive uptake of acetate in the ruminal epithelium of sheep. Am J Physiol Gastrointest Liver Physiol. 2009; 296: G1098–G1107.

Ash R, Baird GD. Activation of volatile fatty acids in bovine liver and rumen epithelium. Biochem J. 1973; 136:311-319.

Atasoglu C, Valdes C, Walker ND, Newbold CJ, Wallace RJ. De novo synthesis of amino acids by the ruminal bacteria *Prevotella bryantii* B 14, *Selenomonas ruminantium* HD4, and *Streptococcus bovis* ES1. Am Soc Microbiol. 1998; 64(8):2836-2843.

Baker SD, Szasz JI, Klein TA, Kuber PS, Hunt CW, Glaze JB, Falk D, Richard R, Miller JC, Battaglia RA, Hill RA. Residual feed intake of purebred Angus steers: effects on meat quality and palatability. J Anim Sci. 2006; 84(4):938-995.

Basarab JA, Price MA, Okine EK. Commercialization of net feed efficiency. Proceedings of the 23rd Western Nutritional Conference, Edmonton, Alberta, Canada. 2002; p.183-194.

Basarab JA, Price MA, Aalhus JL, Okine EK, Snelling WM, Lyle KL. Residual feed intake and body composition in young growing cattle. Can J Anim Sci. 2003; 83:189-204.

Baum B, Georgiou M. Dynamics of adherens junctions in epithelial establishment, maintenance, and remodeling. J Cell Biol. 2011; 192(6):907-917.

Becker HM, Deitmer JW. Nonenzymatic proton handling by carbonic anhydrase II during H+-lactate cotransport via monocarboxylate transporter 1. J Biol Chem. 2008; 283(31):21655-21667.

Bergman EN. Energy contributions of volatile fatty acids from the gastrointestinal tract in various species. Physiol Rev. 1990; 70:567-590.

Bhatta R, Tajima K, Kurihara M. Influence of temperature and pH on fermentation pattern and methane production in the rumen simulating fermenter (RUSITEC). Asian-Aust J Anim Sci. 2006; 19(3):376-380.

Broderick G, Craig M. Metabolism of peptides and amino acids during in vitro protein degradation by mixed rumen organisms. J Dairy Sci. 1989; 72(10):2540-2548.

Canadian Council on Animal Care (CCAC). Olfert ED, Cross BM, McWilliams AA, editors. Guide to the care and use of experimental animals. Vol. 1, 2nd ed. Ottawa, ON: CCAC; 1993.

Castro Bulle FC, Paulino PV, Sanches AC, Sainz RD. Growth, carcass quality, and protein and energy metabolism in beef cattle with different growth potentials and residual feed intakes. J Anim Sci. 2007; 85(4):928-936.

Chen Y, Gondro C, Quinn K, Herd RM, Parnell PF, Vanselow B. Global gene expression profiling reveals genes expressed differentially in cattle with high and low residual feed intake. Anim Genet. 2011; 42:475-490.

Cheng KJ, Wallace RJ. The mechanism of passage of endogenous urea through the rumen wall and the role of ureolytic epithelial bacteria in the urea flux. Brit J Nutr. 1979; 42:553-557.

Cheng KJ, McCowan RP, Costerton JW. Adherent epithelial bacteria in ruminants and their roles in digestive tract function. Am J Clin Nutr. 1979; 32:139-148.

Cheng KJ, Stewart CS, Dinsdale D, Costerton JW. Electron microscopy of bacteria involved in the digestion of plant cell walls. Anim Feed Sci Tech. 1984; 10(2):93-120.

Cottle D, Kahn L. Beef cattle production and trade. Australia: CSIRO Publishing. 2014; p. 221.

Craig WM, Broderick GA, Ricker DB. Quantitation of microorganisms associated with the particulate phase of ruminal ingesta. J Nutr. 1987; 117(1):56-62.

Crowley JJ, McGee M, Kenny DA, Crews Jr. DH, Evans RD, Berry DP. Phenotypic and genetic parameters for different measures of feed efficiency in different breeds of Irish performance-tested beef bulls. J Anim Sci. 2010; 88:885-894.

DeSantis TZ, Hugenholtz P, Larsen N, Rojas M, Brodie EL, Keller K, Huber T, Dalevi D, Hu P, Andersen GL. Greengenes, a chimera-checked 16s rrna gene database and workbench compatible with ARB. Appl Environ Microbiol. 2006; 72(7): 5069-5072. doi: 10.1128/AEM.03006-05

Dijkstra J, Boer H, Van Bruchem J, Bruining M, Tamminga S. Absorption of volatile fatty acids from the rumen of lactating dairy cows as influenced by volatile fatty acid concentration, pH and rumen liquid volume. Brit J Nutr. 1993; 69(02):385-396.

Dijkstra J, Forbes JM, France J. Quantitative aspects of ruminant digestion and metabolism. United Kingdom: CABI publishing. 2005; p.158.

Dinsdale D, Cheng KJ, Wallace RJ, Goodlad RA. Digestion of epithelial tissue of the rumen wall by adherent bacteria in infused and conventionally fed sheep. Appl Environ Microbiol. 1980; 39(5):1059-1066.

Dovas A, Couchman JR. RhoGDI: multiple functions in the regulation of Rho family GTPase activities. Biochem J. 2005; 390:1-9.

Durinck S, Spellman P, Birney E, Huber W. Mapping identifiers for the integration of genomic datasets with the R/Bioconductor package biomaRt. Nat Protoc. 2009; 4:1184–1191.

Durunna ON, Mujibi FD, Goonewardene L, Okine EK, Basarab JA, Wang Z, Moore SS. Feed efficiency differences and reranking in beef steers fed grower and finisher diets. J Anim Sci. 2011; 89(1):158-67.

Fonty G, Gouet P, Jouany JP, Senaud J. Establishment of the microflora and anaerobic fungi in the rumen of lambs. J Gen Microbiol. 1987; 133(7):1835-1843.

Fox DG, Tedeschi LO, Guiroy PJ. Determining feed intake and feed efficiency of individual cattle fed in groups. San Antonio, TX: Beef Improvement Federation. 2001; 11:80-98.

Gentleman RC, Carey VJ, Bates DM, Bolstad B, Dettling M, Dudoit S, Ellis B, Gautier L, Ge Y, Gentry J, Hornik K, Hothorn T, Huber W, Iacus S, Irizarry R, Leisch F, Li C, Maechler M, Rossini AJ, Sawitzki G, Smith C, Smyth G, Tierney L, Yang JYH, Zhang J. Bioconductor: open software development for computational biology and bioinformatics. Genome Biol. 2004; 5:R80.

Golden JW, Kerley MS, Kolath WH. The relationship of feeding behavior to residual feed intake in crossbred Angus steers fed traditional and no-roughage diets. J Anim Sci. 2008; 86(1):180-186.

Goodlad RA. Some effects of diet on the mitotic index and the cell cycle of the ruminal epithelium of sheep. Quart J Exp Physiol. 1981; 66:487-499.

Graham C, Simmons NL. Functional organization of the bovine rumen epithelium. Am J Physiol Regul Integr Comp Physiol. 2005; 288:R173–R181.

Guan LL, Nkrumah JD, Basarab JA, Moore SS. Linkage of microbial ecology to phenotype: correlation of rumen microbial ecology to cattle's feed efficiency. FEMS Microbiol Lett. 2008; 288:85-91.

Guo X, Rao JN, Liu L, Zou T, Turner DJ, Bass BL, Wang J. Regulation of adherens junctions and epithelial paracellular permeability: a novel function for polyamines. Am J Physiol Cell Physiol. 2003; 285:C1174-C1187.

Hadjiagapiou C, Schmidt L, Dudeja PK, Layden TJ, Ramaswamy K. Mechanism(s) of butyrate transport in Caco-2 cells: role of monocarboxylate transporter. Am J Physiol Gastro Physiol. 2000; 279(4):G775-G780.

Hegarty RS, Goopy JP, Herd RM, McCorkell B. Cattle selected for lower residual feed intake have reduced daily methane production. J Anim Sci. 2007; 85(6):1479-1486.

Heisenberg CP, Bellaïche Y. Forces in tissue morphogenesis and patterning. Cell. 2013; 153(5):948-962.

Herd RM, Bishop SC. Genetic variation in residual feed intake and its association with other production traits in British Hereford cattle. Livest Prod Sci. 2000; 63(2):111-119.

Herd RM, Arthur PF. Physiological basis for residual feed intake. J Anim Sci. 2009; 87:E64-E71.

Hernandez-Sanabria E, Guan LL, Goonewardene LA, Li M, Mujibi DF, Stothard P, Moore SS, Leon-Quintero MC. Correlation of particular bacterial PCR-denaturing gradient gel electrophoresis patterns with bovine ruminal fermentation parameters and feed efficiency traits. Appl Environ Microbiol. 2010; 76(19):6338-6350.

Hernandez-Sanabria E, Goonewardene LA, Wang Z, Durunna ON, Moore SS, Guan LL. Impact of feed efficiency and diet on adaptive variations in the bacterial community in the rumen fluid of cattle. Appl Environ Microbiol. 2012; 78(4):1203-1214. doi: 10.1128/AEM.05114-11

Hobson PN, Stewart CS, editors. The rumen microbial ecosystem. Springer Science & Business Media. 1997; p.389.

Holovska K, Lenartova V, Holovska K, Javorsky P. Characterization of superoxide dismutase in the rumen bacterium *Streptococcus bovis*. Vet Med. 2002; 47(2-3):38-44.

Huang DW, Sherman BT, Lempicki RA. Systematic and integrative analysis of large gene lists using DAVID Bioinformatics Resources. Nat Protoc. 2009a; 4(1):44-57.

Huang DW, Sherman BT, Lempicki RA. Bioinformatics enrichment tools: paths toward the comprehensive functional analysis of large gene lists. Nucleic Acids Res. 2009b; 37(1):1-13.

Hvelplund T, Larsen M, Lund P, Weisbjerg MR. Fractional rate of degradation (k_d) of starch in the rumen and its relation to in vivo rumen and total digestibility. South Afri J Anim Sci. 2009; 39(5):133-136.

Jänes J, Hu F, Lewin A, Turro E. A comparative study of RNA-seq analysis strategies. Brief Bioinform. 2015; 16(6):932-940. doi:10.1093/bib/bbv007

Janssen PH, Kirs M. Structure of the archaeal community of the rumen. Appl Environ Microbiol. 2008; 74(12):3619-3625. doi:10.1128/AEM.02812-07

Johnson DE, Ward GM. Estimates of animal methane emissions. Environ Monit Assess. 1996; 42:133-141.

Jurtshuk P, Milligan TW. Quantitation of the tetramethyl-p-phenylenediamine oxidase reaction in *Neisseria* species. Appl Microbiol. 1974; 28(6):1079-1081.

Kamra DN. Rumen microbial ecosystem. Curr Sci. 2005; 89:124–135.

Kanehisa M, Goto S. KEGG: Kyoto encyclopedia of genes and genomes. Nucleic Acids Res. 2000; 28:27-30.

Kanehisa M, Goto S, Sato Y, Kawashima M, Furumichi M, Tanabe M. Data, information, knowledge and principle: back to metabolism in KEGG. Nucleic Acids Res. 2014; 42:D199–D205.

Kang SH, Evans P, Morrison M, McSweeney C. Identification of metabolically active proteobacterial and archaeal communities in the rumen by DNA- and RNA- derived 16S rRNA gene. J Appl Microbiol. 2013; 115(3):644-653.

Karisa BK, Thomson J, Wang Z, Stothard P, Moore SS, Plastow GS. Candidate genes and single nucleotide polymorphisms associated with variation in residual feed intake in beef cattle. J Anim Sci. 2013; 91:3502–3513.

Kelly AK, Waters SM, McGee M, Fonseca RG, Carberry C, Kenny DA. mRNA expression of genes regulating oxidative phosphorylation in the muscle of beef cattle divergently ranked on residual feed intake. Physiol Genomics. 2011; 43:12-23.

Khelaifia S, Raoult D, Drancourt M. A versatile medium for cultivating methanogenic archaea. PLoS One. 2013; 8(4): e61563

Kim D, Pertea G, Trapnell C, Pimentel H, Kelley R, Salzberg SL. TopHat2: accurate alignment of transcriotomes in the presence of insertions, deletions and gene fusions. Genome Biol. 2013; 14:R36. doi: 10.1186/gb-2013-14-4-r36

Klieve AV, Swain RA. Estimation of ruminal bacteriophage numbers by pulsed-field gel electrophoresis and laser densitometry. Appl Environ Microbiol. 1993; 59(7):2299-2303.

Knapp JR, Laur GL, Vadas PA, Weiss WP, Tricarico JM. Invited review: enteric methane in dairy cattle production: quantifying the opportunities and impact of reducing emissions. J Dairy Sci. 2014; 97(6):3231-3261.

Koch RM, Swiger LA, Chambers D, Gregory KE. Efficiency of feed use in beef cattle. J Anim Sci. 1963; 22:486-494.

Kolath WH, Kerley MS, Golden JW, Keisler DH. The relationship between mitochondrial function and residual feed intake in Angus steers. J Anim Sci. 2006; 84:861-865.

Kopylova E, Noe L, Touzet H. SortMeRNA: fast and accurate filtering of ribosomal RNAs in metatranscriptomic data. Bioinform. 2012; 28(24):3211-3217. doi:10.1093/bioinformatics/bts611

Kristensen NB, Danfær A, Tetens V, Agergaard N. Portal recovery of intraruminally infused short-chain fatty acids in sheep. Acta Agri Scand Anim Sci. 1996; 46(1):26-38.

Kristensen NB, Gäbel G, Pierzynowski SG, Danfaer A. Portal recovery of short-chain fatty acids infused into the temporarily-isolated and washed reticulo-rumen of sheep. Brit J Nutr. 2000a; 84(04):477-482.

Kristensen NB, Pierzynowski SG, Danfaer A. Net portal appearance of volatile fatty acids in sheep intraruminally infused with mixtures of acetate, propionate, isobutyrate, butyrate, and valerate. J Anim Sci. 2000b; 78(5):1372-1379.

Kuhn RM, Haussler D, Kent WJ. The UCSC genome browser and associated tools. Brief Bioinform. 2012; 14(2):144-161.

Kurita S, Ogita H, Takai Y. Cooperative role of nectin-nectin and nectin-afadin interactions in formation of nectin-based cell-cell adhesion. J Biol Chem. 2011; 286(42):36297-36303.

Kuroda S, Fukata M, Nakagawa M, Fujii K, Nakamura T, Ookubo T, Izawa I, Nagase T, Nomura N, Tani H, Shoji I, Matsuura Y, Yonehara S, Kaibuchi K. Role of IQGAP1, a target of the small GTPases Cdc42 and Rac1, in regulation of E-Cadherin mediated cell-cell adhesion. Science. 1998; 281:832-835.

Laarman AH, Dionissopoulos L, AlZahal O, Steele MA, Greenwood SL, Matthews JC, McBride BW. Butyrate supplementation affects mRNA abundance of genes involved in glycolysis, oxidative phosphorylation and lipogenesis in the rumen epithelium of Holstein dairy cows. Am J Anim Vet Sci. 2013; 8(4):239-245.

Lancaster PA, Carstens GE, Michal JJ, Brennan KM, Johnson KA, Davis ME. Relationships between residual feed intake and hepatic mitochondrial function in growing beef cattle. J Anim Sci. 2014; 92:3134-3141.

Lane MA, Baldwin RT, Jesse BW. Developmental changes in ketogenic enzyme gene expression during sheep rumen development. J Anim Sci. 2002; 80(6):1538-1544.

Langfelder P, Horvath S. WGCNA: an R package for weighted correlation network analysis. BMC Bioinform. 2008; 9:559. doi:10.1186/1471-2105-9-559

Langmead B, Salzberg SL. Fast gapped-read alignment with Bowtie 2. Nat Methods. 2012; 9(4):357-359.

Lastovica AJ, On SLW, Zhang L. The family *Campylobacteraceae*. The Prokaryotes. Berlin Heidelberg: Springer. 2014; p. 307-335.

Laukova A, Koniarova I. Survey of urease activity in ruminal bacteria isolated from domestic and wild ruminants. Microbios. 1995; 84(338):7-11.

Leahy SC, Kelly WJ, et al. The genome sequence of the rumen methanogen *Methanobrevibacter ruminantium* reveals new possibilities for controlling ruminant methane emissions. PLoS One. 2010; 5(1):e8926.

Leighton B, Nicholas AR, Pogson CI. The pathway of ketogenesis in rumen epithelium of the sheep. Biochem J. 1983; 216:769-772.

Lelieveld JO, Crutzen PJ, Dentener FJ. Changing concentration, lifetime and climate forcing of atmospheric methane. Tellus B. 1998; 50(2):128-150.

Li H, Hansaker B, Wysoker A, Fennell T, Ruan J, Homer N, Marth G, Abecasis G, Durbin R, and 1000 Genome Project Data Processing Subgroup. The sequence alignment/map format and SAMtools. Bioinform. 2009; 25(16):2078-2079.

Li M, Zhou M, Adamowicz E, Basarab JA, Guan LL. Characterization of bovine ruminal epithelial bacterial communities using 16S rRNA sequencing, PCR-DGGE, and qRT-PCR analysis. Vet Microbiol. 2012; 155(1):72-80.

Liu Y, Whitman WB. Metabolic, phylogenetic, and ecological diversity of the methanogenic archaea. Ann N Y Acad Sci. 2008; 1125:171–189. doi:10.1196/annals.1419.019

López S, Hovell FDD, Dijkstra J, France J. Effects of volatile fatty acid supply on their absorption and on water kinetics in the rumen of sheep sustained by intragastric infusions. J Anim Sci. 2003; 81:2609–2616.

Love MI, Huber W, Anders S. Moderated estimation of fold change and dispersion for RNA-seq data with DESeq2. Genome Biol. 2014; 15:550.

Lowe SE, Theodorou MK, Trinci AP. Growth and fermentation of an anaerobic rumen fungus on various carbon sources and effect of temperature on development. Appl Environ Microbiol. 1987; 53(6):1210-1215.

McCarthy RD, Klismeyer TH, Vicini JL, Clark JH, Nelson DR. Effects of source of protein and carbohydrate on ruminal fermentation and passage of nutrients to the small intestine of lactating cows. J Dairy Sci. 1988; 72(8):2002-2016.

McCowan RP, Cheng KJ, Bailey CBM, Costerton JW. Adhesion of bacteria to epithelial cell surfaces within the reticulo-rumen of cattle. Appl Environ Microbiol. 1978; 35(1):149-155.

McDonagh MB, Herd RM, Richardson EC, Oddy VH, Archer JA, Arthur PF. Meat quality and the calpain system of feedlot steers following a single generation of divergent selection for residual feed intake. Anim Prod Sci. 2001; 41(7):1013-1021.

Mi H, Muruganujan A, Thomas PD. PANTHER in 2013: modeling the evolution of gene function, and other gene attributes, in the context of phylogenetic trees. Nucleic Acids Res. 2013; 41(D1):D377-D386.

Morgavi DP, Forano E, Martin C, Newbold CJ. Microbial ecosystem and methanogenesis in ruminants. Anim. 2010; 4(7):1024–1036. doi: 10.1017/S1751731110000546

Moss AR, Jouany JP, Newbold J. Methane production by ruminants: its contribution to global warming. Annal Zootech. 2000; 49(3):231-253.

Mount DB, Romero MF. The SLC26 gene family of multifunctional anion exchangers. Pflügers Arch. 2004; 447(5):710-721.

Murphy MP. How mitochondria produce reactive oxygen species. Biochem J. 2009; 417(1):1-13.

Nathke IS, Hinck L, Swedlow JR, Papkoff J, Nelson WJ. Defining interactions and distributions of cadherin and catenin complexes in polarized epithelial cells. J Cell Biol. 1994; 125(6):1341-1352.

Nayananjalie WAD, Wiles TR, Gerrard DE, McCann MA, Hanigan MD. Acetate and glucose incorporation into subcutaneous, intramuscular, and visceral fat of finishing steers. J Anim Sci. 2015; doi:10.2527/jas2014-8374.

Nkrumah JD, Okine EK, Mathison GW, Schmid K, Li C, Basarab A, Price MA, Wang Z, Moore SS. Relationships of feedlot feed efficiency, performance, and feeding behavior with metabolic rate, methane production, and energy partitioning in beef cattle. J Anim Sci. 2006; 84:145-153.

Obara Y, Shimbayashi K. The appearance of re-cycled urea in the digestive tract of goats during the final third of a once daily feeding of a low-protein ration. Brit J Nutr. 1980; 44(03):295-305.

Okine EK, Basarab JA, Baron V, Price MA. Net feed efficiency in young growing cattle: III. Relationships to methane and manure production. Can J Anim Sci. 2001; 81:614.

Olubobokun JA, Craig WM. Quantity and characteristics of microorganisms associated with ruminal fluid or particles. J Anim Sci. 1990; 68(10):3360-3370.

Owens FN, Gill DR, Secrist DS, Coleman SW. Review of some aspects of growth and development of feedlot cattle. J Anim Sci. 1995; 73(10):3152-3172.

Ozawa M, Ohkubo T. Tyrosine phosphorylation of p120ctn in v-Src transfected L cells depends on its association with E-cadherin and reduces adhesion activity. J Cell Sci. 2001; 114:503-512.

Palacios F, Tushir JS, Fujita Y, D'Souza-Schorey C. Lysosomal targeting of E-cadherin: a unique mechanism for the down-regulation of cell-cell adhesion during epithelial to mesenchymal transitions. Mol Cell Biol. 2005; 25(1):389-402.

Park I, Lee H. EphB/ephrinB signaling in cell adhesion and migration. Mol Cells. 2015; 38(1):14-19.

Paterson AD, Parton RG, Ferguson C, Stow JL, Yap AS. Characterization of E-cadherin endocytosis in isolated MCF-7 and chinese hamster ovary cells. J Biol Chem. 2003; 278(23):21050–21057.

Patterson JA, Hespell RB. Glutamine synthetase activity in the ruminal bacterium *Succinivibrio dextrinosolvens*. Appl Environ Microbiol. 1985; 50(4):1014-1020.

Pei CX, Mao SY, Cheng YF, Zhu WY. Diversity, abundance and novel 16S rRNA gene sequences of methanogens in rumen liquid, solid and epithelium fractions of Jinnan cattle. Anim. 2010; 4(01):20-29.

Perkins SD, Key CN, Garrett CF, Foradori CD, Bratcher CL, Kriese-Anderson LA, Brandebourg TD. Residual feed intake studies in Angus-sired cattle reveal a potential role for hypothalamic gene expression in regulating feed efficiency. J Anim Sci. 2014; 92:549-560.

Peters JP, Shen RY, Robinson JA, Chester ST. Disappearance and passage of propionic acid from the rumen of the beef steer. J Anim Sci. 1990; 68(10):3337-3349.

Peters JP, Shen RY, Robinson JA. Disappearance of acetic acid from the bovine reticulorumen at basal and elevated concentrations of acetic acid. J Anim Sci. 1992; 70(5):1509-1517.

Piedra J, Martinez D, Castano J, Miravet S, Dunach M, and Herreros AG. Regulation of β-catenin structure and activity by tyrosine phosphorylation. J Biol Chem. 2001; 276(23):20436-20443.

Pilgrim AF, Gray FV, Weller RA, Belling CB. Synthesis of microbial protein from ammonia in the sheep's rumen and the proportion of dietary nitrogen converted into microbial nitrogen. Brit J Nutr. 1970; 24:589-598.

R Core Team. R: A language and environment for statistical computing. R Foundation for Statistical Computing, Vienna, Austria. 2014. http://www.R-project.org/.

Rekawiecki R, Rutkowska J, Kotwica J. Identification of optimal housekeeping genes for examination of gene expression in bovine corpus luteum. Reprod Biol. 2012; 12:362-367.

Richardson EC, Kilgour RJ, Archer JA, Herd RM. Pedometers measure differences in activity in bulls selected for high or low net feed efficiency. Proc Aust Soc Study Anim Behav. 1999; 26:16.

Richardson EC, Herd RM, Oddy VH, Thompson JM, Archer JA, Arthur PF. Body composition and implications for heat production of Angus steer progeny of parents selected for and against residual feed intake. Aust J Exp Agric. 2001; 41(7):1065-1072.

Richardson EC, Herd RM, Colditz IG, Archer JA, Arthur PF. Blood cell profiles of steer progeny from parents selected for and against residual feed intake. Anim Prod Sci. 2002; 42(7):901-908.

Richardson EC, Herd RM. Biological basis for variation in residual feed intake in beef cattle. 2. Synthesis of results following divergent selection. Aust J Exp Agr. 2004; 44:431-440.

Ridley AJ. Rho GTPases and cell migration. J Cell Sci. 2001; 114:2713-2722.

Robinson AM, Williamson DH. Physiological roles of ketone bodies as substrates and signals in mammalian tissues. Physiol Rev. 1980; 60(1):143-187.

Romero MF, Fulton CM, Boron WF. The SLC4 family of HCO3− transporters. Pflügers Arch. 2004; 447(5):495-509.

Rosegrant MW. Biofuels and grain prices: impacts and policy responses. Washington, DC: International Food Policy Research Institute. 2008; p.1-4.

Samuel BS, Hansen EE, et al. Genomic and metabolic adaptations of *Methanobrevibacter smithii* to the human gut. Proc Natl Acad Sci. 2007; 104(25):10643-10648.

Schloss PD, Westcott SL, Ryabin T, Hall JR, Hartmann M, Hollister EB, Lesniewski RA, Oakley BB, Parks DH, Robinson CJ, Sahl JW, Stres B, Thallinger GG, Van Horn DJ, Weber CF. Introducing mothur: open-source, platform-independent, community-supported software for describing and comparing microbial communities. Appl Environ Microbiol. 2009; 75(23):7537-7541. doi:10.1128/AEM.01541-09

Schwab EC, Schwab CG, Shaver RD, Girard CL, Putnam DE, Whitehouse NL. Dietary forage and nonfiber carbohydrate contents influence B-vitamin intake, duodenal flow, and apparent ruminal synthesis in lactating dairy cows. J Dairy Sci. 2006; 89:174-187.

Seedorf H, Kittelmann S, Janssen PH. Few highly abundant operational taxonomic units dominate within rumen methanogenic archaeal species in New Zealand sheep and cattle. Appl Environ Microb. 2015; 81(3):986-995.

Sehested J, Diernæs L, Møller PD, Skadhauge E. Ruminal transport and metabolism of short-chain fatty acids (SCFA) in vitro: effect of SCFA chain length and pH. Comp Biochem Physiol. 1999; 123:359-368.

Shin EC, Choi BR, Lim WJ, Hong SY, An CL, Cho KM, Kim YK, An JM, Kang JM, Lee SS, Kim H, Yun HD. Phylogenetic analysis of archaea in three fractions of cow rumen based on the 16S rDNA sequence. Anaerobe. 2004; 10(6):313-319.

Singh KM, Tripathi AK, Pandya PR, Parnerkar S, Kothari RK, Joshi CG. Molecular genetic diversity and quantitation of methanogen in ruminal fluid of buffalo (Bubalus bubalis) fed ration (wheat straw and concentrate mixture diet). Genet Res Int. 2013; 2013:1-7.

Speicher DJ, Johnson NW. Detection of human herpesvirus 8 by quantitative polymerase chain reaction: development and standardisation of methods. BMC Infect Dis. 2012; 12:210.

Stackebrandt E, Hespell RB. The family *Succinivibrionaceae*. The Prokaryotes. New York: Springer. 2006; p. 419-429.

Steele MA, Croom J, Kahler M, AlZahal O, Hook SE, Plaizier K, McBride BW. Bovine rumen epithelium undergoes rapid structural adaptations during grain-induced subacute ruminal acidosis. Am J Physiol Regul Integr Comp Physiol. 2011; 300:R1515–R1523.

Sues HD. Evolution of herbivory in terrestrial vertebrates: perspectives from the fossil record. New York: Cambridge University Press. 2005; p.2.

Takeichi M. Cadherins: a molecular family important in selective cell-cell adhesion. Annu Rev Biochem. 1990; 59:237-252.

Tilman D, Balzer C, Hill J, Befort BL. Global food demand and the sustainable intensification of agriculture. Proc Nat Acad Sci. 2011; 108(50):20260-20264.

Thoreson MA, Anastasiadis PZ, Daniel JM, Ireton RC, Wheelock MJ, Johnson KR, Hummingbird DK, Reynolds AB. Selective uncoupling of p120ctn from e-cadherin disrupts strong adhesion. J Cell Biol. 2000; 148:189-201.

Troyanovsky RB, Sokolov EP, Troyanovsky SM. Endocytosis of cadherin from intracellular junctions is the driving force for cadherin adhesive dimer disassembly. Mol Biol Cell. 2006; 17: 3484–3493.

United Nations. The World Population Situation in 2014. Department of economic and social affairs population division. 2014; p.1-30.

Van Soest PJ. Nutritional ecology of the ruminant. New York: Cornell University Press. 1994; p. 224, 236-237, 314.

Vasioukhin V, Bauer C, Yin M, Fuchs E. Directed actin polymerization is the driving force for epithelial cell-cell adhesion. Cell. 2000; 100:209-219.

Wahrmund JL, Ronchesel JR, Krehbiel CR, Goad CL, Trost SM, Richards CL. Ruminal acidosis challenge impact on ruminal temperature in feedlot cattle. J Anim Sci. 2012; 90:2794-2801.

Walter J, Tannock GW, Tilsala-Timisjarvi A, Rodtong S, Loach DM, Munro K, Alatossava T. Detection and identification of gastrointestinal *Lactobacillus* species by using denaturing gradient gel electrophoresis and species-specific PCR primers. Appl Environ Microbiol. 2000; 66:297–303.

Wellen KE, Thompson CB. Cellular metabolic stress: considering how cells respond to nutrient excess. Mol Cell. 2010; 40(2):323-332.

Wolin MJ. The rumen fermentation: a model for microbial interactions in anaerobic ecosystems. Adv Microb Ecol. 1979; 3:49-77.

Yan L, Zhang B, Shen Z. Dietary modulation of the expression of genes involved in short-chain fatty acid absorption in the rumen epithelium is related to short-chain fatty acid concentration and pH in the rumen of goats. J Dairy Sci. 2014; 97(9):5668-5675.

Yue X, Dechow C, Chang T, DeJarnette JM, Marshall CE, Lei C, Liu W. Copy number variations of the extensively amplified Y-linked genes, HSFY and ZNF280BY, in cattle and their association with male reproductive traits in Holstein bulls. BMC Genom. 2014; 15:113.

Zhang Y, Gao W, Meng Q. Fermentation of plant cell walls by ruminal bacteria, protozoa and fungi and their interaction with fibre particle size. Arch Anim Nutr. 2007; 61(2):114-125.

Zhou M, Hernandez-Sanabria E, Guan LL. Assessment of the microbial ecology of ruminal methanogens in cattle with different feed efficiencies. Appl Environ Microbiol. 2009; 75(20):6524-6533.

Zhou M, Hernandez-Sanabria E, Guan LL. Characterization of variation in rumen methanogenic communities under different dietary and host feed efficiency conditions, as determined by PCR-denaturing gradient gel electrophoresis analysis. Appl Environ Microbiol. 2010; 76(12):3776-3786.